Agricultural Water Management 288 (2023) 108487

Contents lists available at ScienceDirect

Agricultural Water Management

journal homepage: www.elsevier.com/locate/agwat

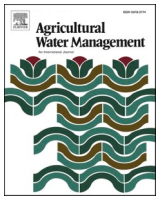

Root traits and resource acquisition determining durum wheat performance under Mediterranean conditions: An integrative approach

Fatima Zahra Rezzouk [a,b], Adrian Gracia-Romero [a,b], Joel Segarra [a,b], Shawn C. Kefauver [a,b], Nieves Aparicio [c], Maria Dolors Serret [a,b], José Luis Araus [a,b,*]

[a] Integrative Crop Ecophysiology Group, Plant Physiology Section, Faculty of Biology, University of Barcelona, Spain
[b] AGROTECNIO (Center for Research in Agrotechnology), Lleida, Spain
[c] Agro-technological Institute of Castilla y León (ITACyL), Valladolid, Spain

ARTICLE INFO

Handling Editor: Dr. B.E. Clothier

Keywords:
Soil coring
Shovelomics
Stable isotopes
Canopy temperature

ABSTRACT

Crop performance is very dependent on roots because they determine the capture of water and nutrients, and the crop's subsequent growth and productivity. Durum wheat is a major crop in the Mediterranean region, where water and nitrogen availability limit its productivity. Therefore, the focus of this study was to uncover the response of root and shoot traits in durum wheat to different Mediterranean growing conditions and how they relate to better growth and yield performance. For this purpose, crop performance was evaluated in a set of modern durum wheat cultivars grown during four consecutive seasons and under contrasting water regimes, temperatures and nitrogen supplies, totalling 12 different growing conditions. Grain yield, biomass, other crop-growth traits (plant height, PH, and the Normalised Difference Vegetation Index, NDVI), together with physiological indicators of water (carbon isotope composition, $\delta^{13}C$, and canopy temperature depression, CTD) and nitrogen (nitrogen isotope composition, $\delta^{15}N$, and grain nitrogen yield, GNY) status were assessed. In addition, root architecture and distribution were measured using shovelomics and soil coring, and the provenance of the water captured by roots was determined by comparing the oxygen ($\delta^{18}O$) and hydrogen ($\delta^{2}H$) isotope compositions of water at the base of the stem, with water in different soil sections. Water and nitrogen status indicators combined with shovelomic traits allowed development of yield-prediction models. while higher yields were associated in most cases with better water status, root architecture was very responsive to different growing conditions. Overall, genotypes better adapted to rainfed conditions exhibited roots favouring deeper water extraction, whereas under support irrigation, the root system enabled water extraction from the topsoil as from deeper soil sections. Our study also highlights the limitation of shovelomics and soil coring as phenotyping approaches and proposes the $\delta^{18}O$ of stem water as a promising functional phenotypic approach.

1. Introduction

Durum wheat is a major crop in the Mediterranean basin, encompassing more than 50 % of the total wheat growing area (Guzmán et al., 2016). It is grown mainly under rainfed conditions and used in the production of various staple food in the Mediterranean region (Dainelli et al., 2022; Xynias et al., 2020). Mediterranean climatic conditions are known for their high annual variability with fluctuating precipitation and temperatures (Hoffmann et al., 2018). Moreover, climatic projections forecast that a warmer and drier climate across the Mediterranean will increase the risk of yield loss in durum wheat (Ceglar et al., 2021; Ferrise et al., 2011). In addition, nitrogen availability is also a

Abbreviations: $\delta^{2}H$, hydrogen isotope composition; $\delta^{13}C$, carbon isotope composition; $\delta^{15}N$, nitrogen isotope composition; $\delta^{18}O$, oxygen isotope composition; Bush, root network bushiness; ConvA, root network convex area; CTD, canopy temperature depression; CVD, cryogenic vacuum distillation; GNY, grain nitrogen yield; GY, grain yield; NDVI, normalised difference vegetation index; HI, harvest index; ILP, irrigated late planting; INP, irrigated normal planting; Ldist, root length distribution; MaxR, maximum root number; MedR, median root number; Ndepth/Nlen, root network length; N_{grain}, nitrogen content in grains; N_{leaf}, nitrogen content in leaf; Nsurf, root network surface area; Nvol, root network volume; NwA, root network area; NWDR, root network width to depth ratio; Nwidth, root network width; RA, root angle; Rccomp, root number of connected components; RDW, root dry weight; RF, random forest; RNP, rainfed normal planting; RLN, rainfed normal planting and low nitrogen; Rwidth, root width; PH, plant height; SRL, specific root length; TKW, thousand kernel weight..

* Corresponding author at: Integrative Crop Ecophysiology Group, Plant Physiology Section, Faculty of Biology, University of Barcelona, Spain.
E-mail address: jaraus@ub.edu (J.L. Araus).

https://doi.org/10.1016/j.agwat.2023.108487
Received 6 July 2023; Received in revised form 16 August 2023; Accepted 19 August 2023
Available online 22 August 2023

major factor limiting yield in many Mediterranean areas (Cossani et al., 2010; Savin et al., 2019). With food demands continuing to grow amid population increase, wheat breeders and producers are thus challenged by and expected to overcome these climatic limitations and secure higher production with fewer resources.

Crop growth and its subsequent yield depend on the effective acquisition of resources from the soil, namely water and nutrients. While the crucial role of the root system in determining crop performance is evident, studying roots under field conditions has been limited by the lack of precise high-throughput phenotypic approaches (Vadez, 2014; Wasson et al., 2014). Nevertheless, the root system may provide further understanding about plant coping mechanisms during growth under the drought, high temperature and/or low fertility conditions encountered by Mediterranean agriculture. Therefore, deepening our understanding of how root architecture and function respond to a wide range of growing conditions is necessary to provide insights into root characteristics suitable for tailoring higher yielding cultivars with better adaptation to Mediterranean conditions, and to design more efficient crop management practices. Despite the evident limitations of the current methods for root phenotyping in the field, combining even low throughput methodologies may still provide comprehensive information on root traits when aiming to characterise ideotypes and the effect of crop management conditions.

The wheat root system is characterised by seminal roots that stem from the seed, and nodal or adventitious roots that initiate after germination (Chochois et al., 2015; Maccaferri et al., 2016). Throughout the crop growth cycle, both seminal and nodal roots spread in the soil in horizontal and vertical directions, giving rise to a fibrous system that reaches its optimum growth by anthesis (Barraclough and Weir, 1988; Fageria and Moreira, 2011; Foulkes et al., 2009). Although phenotyping for root traits remains a real challenge given its laborious, destructive and costly nature, several techniques that seek to unveil root characteristics in the field are in use, such as shovelomics and soil coring (Araus et al., 2022; Bucksch et al., 2014; Lynch, 1995, 2013; Ober et al., 2021; Trachsel et al., 2013; Wasson et al., 2014; York et al., 2018a, 2018b). The former is an approach that studies roots in the upper soil layer and defines root crown architecture characteristics (Bucksch et al., 2014; Fradgley et al., 2020; Rezzouk et al., 2022; Wasson et al., 2016). The latter targets root distribution throughout the soil profile, (Box, Ramseur, 1993; Hodgkinson et al., 2017; Kätterer et al., 1993; Kirkegaard and Lilley, 2007; Wasson et al., 2014). Thus, root architecture and growth characteristics such as root depth, angle, density, diameter and specific length have been studied to explain the mechanisms that facilitate drought stress tolerance, and that allow the capture of nutrients and water from the soil and therefore contribute to higher grain yield (Foulkes et al., 2009; He et al., 2022; Narayanan et al., 2014; Rezzouk et al., 2022; York et al., 2018a, 2018b). Nevertheless, adding phenotyping information such as root functionality at the soil depth of water extraction may provide a more comprehensive view of how roots contribute to crop adaptation. In this sense, hydrogen (δ^2H) and oxygen ($\delta^{18}O$) isotope compositions in stem water have been reported to reflect the isotopic signature of the water source (e.g. precipitation and/or irrigation) together with the depth in the soil profile from which the water is captured by the roots (Berry et al., 2019; Dawson and Goldsmith, 2018; de Deurwaerder et al., 2020; Schreel and Steppe, 2020; Treydte et al., 2014; Wang et al., 2010; Zhao et al., 2016). Nevertheless, the use of stem water δ^2H and $\delta^{18}O$ as tracers of the water source must be interpreted with caution, particularly in the case of δ^2H, in which variations between the stem water and the water source have been reported (Barbeta et al., 2022; Chen et al., 2020). Because the functioning of the roots determines the overall performance of the crop (Lopes and Reynolds, 2010; Pinto and Reynolds, 2015), assessing traits that inform about the water and nutrient status of the crop may further improve our mechanistic understanding of the key root traits while facilitating more efficient phenotyping. In terms of nutrient status, a crop capable of assimilating more nitrogen should translate to a higher grain nitrogen yield (GNY), while also increasing the nitrogen content of the leaves (Chairi et al., 2020; Haberle et al., 2008; Rezzouk et al., 2020, 2022; Slafer et al., 1990), as well as the stable nitrogen isotope composition ($\delta^{15}N$) of the plant tissues (Choi et al., 2003; Wassenaar, 1995). Regarding water status, canopy temperature depression (CTD) is a relevant parameter that is used to quantify crop water status, which is related to root performance under field conditions (Lopes and Reynolds, 2010). CTD was reported to be positively correlated with photosynthetic traits such as stomatal conductance and leaf water potential (Wasaya et al., 2018), as well as grain yield (Fischer et al., 1998; Chairi et al., 2020; Wasaya et al., 2018). On the other hand, the stable isotope composition ($\delta^{13}C$) (Farquhar et al., 1989; Farquhar and Richards, 1984) when analysed in plant tissues such as mature grains, it has been frequently used in wheat as a time-integrative indicator of the water used by plants (Araus et al., 2003, 2008), which is also known as the effective use of water (Blum, 2009). In fact, for wheat, the lower the $\delta^{13}C$ values of plant tissues, the better the water status of the crop and the higher the grain yield achieved (Araus et al., 2003, 2013).

Finally, a better water and nutrient status will translate to a higher crop growth and stay green (Christopher et al., 2016; Fischer, 2011; Padovan et al., 2020; Rezzouk et al., 2020; Spano et al., 2003). Canopy height at anthesis/grain filling (Blum and Sullivan, 1997; de Vita et al., 2010), together with the green canopy biomass inferred through remote sensing vegetation indices such as the Normalised Difference Vegetation Index (NDVI) may also be useful as indicators (Christopher et al., 2014; Fischer et al., 1998; Kipp et al., 2014; Lopes and Reynolds, 2012).

Basing the approach on traits that inform about crop growth and water and nitrogen status, and combining those with a wide range of root traits may prove a rigorous way to define ideotypes adapted to Mediterranean conditions and to develop prediction-models amenable for crop management and breeding. Therefore, the objective of this study was to uncover the response of root traits in durum wheat to different Mediterranean growing conditions and how they relate to plant growth, crop stay green, yield performance and the impact of water and nitrogen resource use throughout the crop cycle. Different methodologies examining root architecture in the topsoil (shovelomics) as well as at depth (soil coring) were deployed alongside a functional approach (isotope signature of the stem water) under field conditions. Thus, the rationale is that a more efficient root system will translate to better crop water status (higher CTD and lower $\delta^{13}C$) and nitrogen status (higher GNY, $\delta^{15}N$ and leaf N), greater growth (taller plants) and more stay green (higher NDVI), and as a result, higher yield. Twelve trials, with contrasting water (rainfed vs irrigated), temperature (normal vs late planting) and nitrogen (low versus recommended N fertilisation) conditions were carried out through four consecutive crop seasons under the continental Mediterranean conditions of Valladolid, Spain. A set of modern durum wheat cultivars with contrasting yield performance were evaluated. In conjunction with grain yield and the above-mentioned indicators of crop growth and water and nitrogen status, shovelomics was carried out for all genotypes and trials, and soil coring as well as measurements of the stable isotopic signature of the stem and soil water were undertaken in a subset of seasons.

2. Materials and Methods

2.1. Plant material, field experiment and growth conditions

Field trials were carried out over four consecutive crop seasons (2017–2018, 2018–2019, 2019–2020 and 2020–2021) at the experimental station of Zamadueñas of the Agro-technological Institute of Castilla y León (ITACyL), Valladolid, Spain (41° 39 ´8`N and 4 ° 43`24`` W, 690 m.a.s.l.). For each season, six to eight semi-dwarf durum wheat (*Triticum turgidum* L. subsp. *durum* (Desf) Husn.) post green revolution cultivars were selected according to grain yield data from a panel of 24 modern durum wheat cultivars grown in Spain during the last five decades. Genotype selection was based on the grain yields achieved during

different seasons at the ITACyL station stated above, and at the Spanish stations of INIA "Instituto Nacional de Investigación y Tecnología Agraria y Alimentaria" located in Colmenar de Oreja-Aranjuez (Madrid) and Coria del Rio (Seville), under different growing conditions: irrigated normal planting (INIA, Coria del Rio); irrigated normal planting, irrigated late planting and rainfed normal planting conditions (INIA, Aranjuez); and irrigated normal planting, rainfed normal planting and rainfed normal planting and low nitrogen trials (ITACyL, Valladolid). Briefly, for the first two seasons of this study (2017–2018 and 2018–2019), six genotypes out of twenty-four were selected from yield data obtained at the INIA stations (Aranjuez and Coria del Rio) during the seasons 2016–2017, 2017–2018 and 2018–2019, totalling twelve growth conditions (i.e. environments). During the third season of this study (2019–2020), eight genotypes were selected from yield data collected at the INIA stations (Aranjuez and Coria del Rio) and ITACyL station (Valladolid) from the season 2018–2019, totalling eight environments. In the fourth season (2020–2021), six genotypes were selected from yield data obtained at the INIA station (Aranjuez) from the seasons 2017–2018 and 2018–2019, and the ITACyL station (Valladolid) from the seasons 2017–2018, 2018–2019 and 2019–2020, totalling sixteen environments. Information of the chosen genotypes in each season and their provenances is provided in Supplemental Table 1 as well as elsewhere (Chairi et al., 2018; Rezzouk et al., 2022). In fact, for each of the trials in this study, the tested cultivars were grown within the panel of 24 genotypes, designed in a complete block design with three replicates. In all seasons and for each trial, cultivars were sown in six rows, 0.25 m apart plots, and planting density consisted of 250 seeds per m^2. Plot size was 1.5 m x 7 m during 2017–2018, 1.5 m x 9 m during 2018–2019, and 1.5 m x 10 m during 2019–2020 and 2020–2021. The following growing conditions were tested: support irrigation normal planting (INP), support irrigation late planting (ILP), rainfed normal planting and low nitrogen (RLN), and rainfed normal planting (RNP) (Table 1). Each season consisted of three different growing conditions: INP, RNP and RLN during the seasons 2017–2018 and 2018–2019; INP, ILP and RLN during 2019–2020; and INP, ILP and RNP during 2020–2021; totalling twelve tested environments. During the first two seasons (2017–2018 and 2018–2019), all trials (INP, RLN and RNP) received 300 kg ha^{-1} of 8–15–15 as basic-dressing, and afterwards the INP and RNP trials received 150 kg ha^{-1} of calcium ammonium nitrate (NAC 27 %) as a first top-dressing during tillering, and another 150 kg ha^{-1} of nitrosyl sulfuric acid (NSA 26 %) as a second top-dressing during jointing. During the second two seasons (2019–2020 and 2020–2021),

Table 1
Effects of crop season (2017-2018; 2018-2019; 2019-2020; 2020-2021), trial (INP, ILP, RNP, RLN), and durum wheat genotypes on yield components. ANOVA was tested for trials and genotypes in each crop season and across combined crop seasons.

Crop season	Trial	GY (Mg ha^{-1})	Biomass (Mg ha^{-1})	HI	TKW (g)	Plants (m^{-2})	Ears (m^{-2})	PH (cm)	NDVI
2017–2018	INP	6.16a± 0.26	13.94a± 0.62	0.441a± 0.011	48.15a± 1.44	170.4a± 7.0	351.1a± 15.1	100.4a± 1.3	0.73a± 0.01
	RNP	5.85ab± 0.17	12.89a± 0.33	0.455a± 0.010	47.63a± 1.13	178.9a± 9.9	328.4a± 11.7	99.4a± 1.2	0.67a± 0.01
	RLN	4.93b± 0.38	10.88b± 0.75	0.451a± 0.014	49.36a± 1.26	142.0b± 7.4	325.3a± 17.4	90.3b± 1.9	0.61b± 0.02
	Trial (T)	< 0.050	< 0.010	ns	ns	< 0.010	ns	< 0.001	< 0.001
	Genotype (G)	ns	ns	< 0.001	< 0.001	< 0.050	< 0.010	< 0.001	ns
	TxG	ns	ns	ns	ns	ns	ns	ns	ns
2018–2019	INP	7.88a± 0.24	15.41a± 0.70	0.403a± 0.010	46.11a± 1.85	208.9a± 12.9	417.6a± 19.5	86.88a± 1.24	0.49a± 0.02
	RNP	2.96b± 0.14	7.15b± 0.35	0.294b± 0.015	40.93a± 10.13	182.2a± 7.2	305.6b± 15.9	68.99b± 1.38	0.43b± 0.02
	RLN	2.76b± 0.17	7.04b± 0.52	0.297b± 0.014	31.38a± 1.65	188.7a± 14.3	397.3b± 23.0	67.06b± 2.13	-
	Trial (T)	< 0.001	< 0.001	< 0.001	ns	ns	< 0.001	< 0.001	< 0.050
	Genotype (G)	ns	ns	< 0.010	ns	ns	< 0.010	ns	ns
	TxG	ns	< 0.010	ns	ns	ns	ns	ns	ns
2019–2020	INP	8.36a± 0.18	-	-	-	-	-	104.8a± 1.3	0.75a± 0.01
	ILP	5.43c± 0.16	-	-	-	-	-	100.2b± 1.5	0.67b± 0.01
	RLN	6.04b± 0.30	-	-	-	-	-	100.3b± 0.9	0.58c± 0.02
	Trial (T)	< 0.001	-	-	-	-	-	< 0.001	< 0.001
	Genotype (G)	< 0.001	-	-	-	-	-	< 0.001	< 0.001
	TxG	< 0.010	-	-	-	-	-	< 0.001	< 0.001
2020–2021	INP	6.31a± 0.14	-	-	52.02a± 0.90	171.1a± 7.8	321.2a± 13.4	92.28a± 1.12	0.68b± 0.02
	ILP	4.82b± 0.11	-	-	48.98b± 1.14	185.7a± 5.1	309.4a± 7.6	77.03c± 0.90	0.74a± 0.01
	RNP	4.52b± 0.17	-	-	42.39c± 0.95	171.8a± 4.5	308.5a± 7.5	87.94b± 0.98	0.61c± 0.01
	Trial (T)	< 0.001	-	-	< 0.001	ns	ns	< 0.001	< 0.001
	Genotype (G)	< 0.001	-	-	< 0.001	ns	ns	< 0.050	ns
	TxG	< 0.001	-	-	ns	ns	ns	< 0.010	ns
All seasons	INP	7.26a± 0.15	14.17a± 0.48	0.42a± 0.01	48.76a± 0.90	183.5a± 6.1	364.0a± 10.9	96.77a± 0.10	0.67b± 0.01
	ILP	5.17b± 0.11	-	-	48.98a± 1.14	185.7a± 5.1	309.4b± 7.6	90.60b± 2.03	0.70a± 0.01
	RLN	4.75c± 0.25	9.02b± 0.57	0.38b± 0.02	40.63a± 1.84	164.7a± 8.8	315.8b± 12.3	87.65c± 2.01	0.59c± 0.01
	RNP	5.19b± 0.19	10.02b± 0.54	0.37b± 0.02	43.65a± 3.43	177.6a± 4.4	320.1b± 7.2	90.68b± 1.59	0.60c± 0.01
	Season (S)	< 0.001	< 0.001	< 0.001	ns	ns	ns	< 0.001	< 0.001
	Trial (T)	< 0.001	< 0.001	< 0.050	ns	ns	< 0.010	< 0.001	< 0.001
	Genotype (G)	< 0.010	ns	ns	ns	ns	ns	< 0.010	ns
	SxT	< 0.001	< 0.001	< 0.001	ns	ns	< 0.050	< 0.001	< 0.050
	SxG	< 0.010	ns	ns	ns	ns	< 0.050	ns	ns
	TxG	< 0.050	ns	ns	ns	ns	ns	ns	ns
	SxTxG	ns	ns	ns	ns	ns	ns	ns	ns

Values are means of the selected genotypes in each season with three replicates. Levels of significance for the ANOVA: $P < 0.05$, $P < 0.01$ and $P < 0.001$. Means exhibiting different letters a, b and c, are significantly different ($P < 0.05$) according to Student's t-test on independent samples, within each crop season and across combined seasons. GY, grain yield; HI, harvest index; TKW, thousand kernel weight; PH, plant height; NDVI, nitrogen difference vegetation index; CTD, canopy temperature depression; INP, irrigated normal planting. ILP, irrigated late planting. RNP, rainfed normal planting. RLN, rainfed low nitrogen. S, crop season. T, trial. G, genotype.

the INP, ILP and RNP trials were supplied with 300 kg ha^{-1} of 8–15–15 as basic dressing, and afterwards the INP and RNP trials received 150 kg ha^{-1} of calcium ammonium nitrate (NAC 27 %) during tillering as top-dressing, and ILP received the same top-dressing fertilisation during the 2019–2020 season (Table 1). In terms of phytosanitary treatment, pests, diseases and weeds were treated as recommended by the farmers of the region. Soil was xerofluvent with a sandy loam texture and alkaline pH. Regarding the water regimen, spring irrigation was applied to the irrigated trials (INP and ILP). Each received a total of 109.8 mm divided over eight applications during 2017–2018, 152.7 mm divided over thirteen applications during 2018–2019, 66.0 mm divided over four applications during 2019–2020, and 71.0 mm divided over nine applications during 2020–2021. The accumulated precipitation for normal planting trials (INP, RLN and RNP) totalled 443.8 mm, 124.7 mm, 348.5 mm and 186.5 mm during the four consecutive seasons, respectively. For the ILP, accumulated precipitation was 217.9 mm and 94.2 mm during 2019–2020 and 2020–2021, respectively. Further information on the fertilisation calendar, water input, sowing and harvest dates are detailed in Table 1 while climate conditions for each crop season are presented in Fig. 1.

2.2. Agronomic and crop growth traits

At anthesis, plant height (PH) was determined across the whole plot using a ruler, and the NDVI was measured using a potable ground sensor (GreenSeeker, Trimble, Sunnyvale, CA, USA), following the protocol described previously in Rezzouk et al. (2020). At maturity, plant density (plants m^{-2}) and ear density (ears m^{-2}) were determined by counting the number of plants and ears in a 1 m length of a central row. Afterwards, each plot was machine harvested and grain yield (GY) was determined after an adjustment to a 10 % moisture level. Total biomass was measured for each plot in a subset of 10 plants. Then, thousand kernel weight (TKW) was determined after harvest for each plot in a subsample of seeds and the harvest index (HI) was determined at physiological maturity as grain yield divided by the aboveground biomass.

2.3. Canopy temperature depression

Measurements of canopy temperature (CT) were assessed during the seasons 2017–2018, 2018–2019 and 2020–2021 from an aerial platform using a thermal camera (FLIR Tau2 640, FLIR Systems, Nashua, NH, USA) with a VOx uncooled microbolometer equipped with a TeAx Thermal Capture 2.0 (TeAx Technology, Wilnsdorf, Germany), and mounted on an unmanned aerial vehicle (6S12 XL oktokopter, HiSystems GmbH, Moomerland, Germany). During 2019–2020, CT was assessed at ground level using a portable infrared thermometer (PhotoTempTM MXSTM TD Raytek®, California; USA). In all cases, measurements took place between solar noon and early afternoon. Initially, the thermal frames were stacked to raw 16-bit TIFF format images (temperature values expressed in Kelvin x 10000) using ThermoViewer software (v1.3.13) by TEAX (TeAx Technology, Wilnsdorf, Germany). Secondly, images were 3D-reconstructed using Agisoft Photoscan Pro (Agisoft LLC, St. Petersburg, Russia, http://www.agisoft.com) and processed to produce ortho-mosaic images (Bendig et al., 2014). Thirdly, plots were cropped and aerial CT analysed using the MosaicTool software integrated as a plugin for the open source image analysis platform FIJI (Fiji is Just ImageJ; http://fiji.sc/Fiji), then converted to 32-bit temperatures in Celsius using a custom batch processing macro function in FIJI (Kefauver et al., 2017) to determine aerial CT. Afterwards, canopy temperature depression (CTD) for each plot, trial and crop season was calculated as the difference between the maximum air temperature of the day and the canopy temperature CT measured during the same day as follows:

$$CTD = T_{air} - CT \quad (1)$$

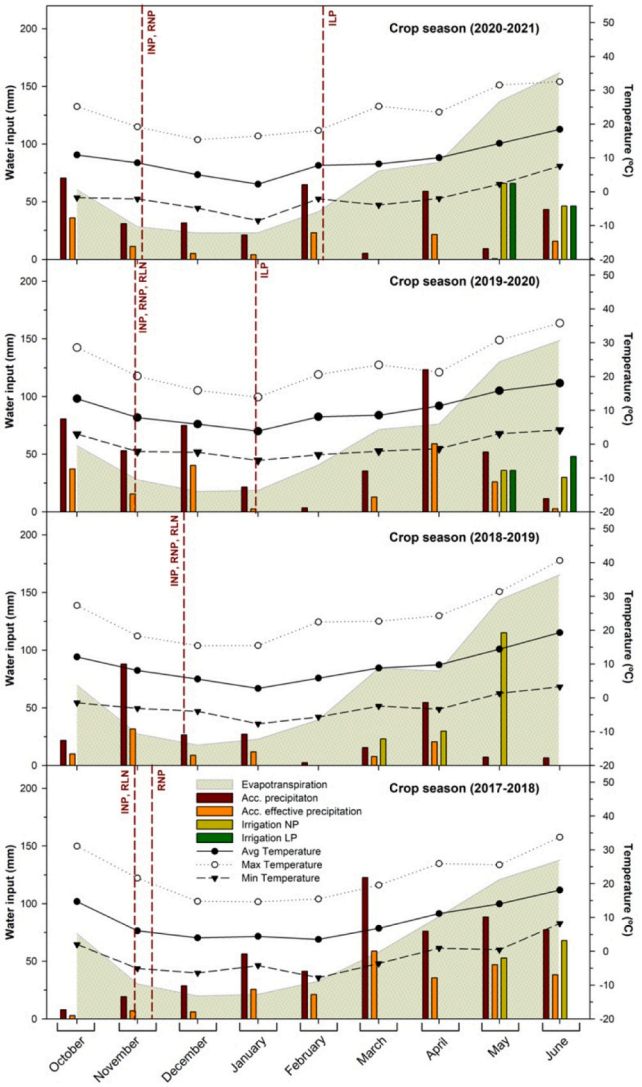

Fig. 1. Distribution of monthly water input (accumulated precipitation, accumulated effective precipitation and irrigation and evapotranspiration), and mean temperature (average, minimum and maximum) during the growing period covering the crop seasons (2017–2018), (2018–2019) and (2019–2020). Climatic conditions were obtained from the Agro-climatic Information System for Irrigation (Sistema de Información Agroclimática para el Regadío, SIAR) (http://eportal.magrama.gob.es/websiar/); Ministry of Agriculture, Food and Environment, Government of Spain and the European Agricultural Fund for Rural Development.

2.4. Shovelomics, soil coring and image processing

For all trials and crop seasons, five random plants were dug manually from the upper 20 cm of soil layer in each plot between anthesis and mid-grain filling. Afterwards, roots of individual plants were washed carefully using a hose, digitised in situ using a Sony ILCE-QX1 camera (Sony Europe Limited, Brooklands; United Kingdom), and the resulting RGB images were processed using GiaRoots software (General Image Analysis of Roots, Georgia Tech Research Corporation and Duke University; USA) as described in Galkovskyi et al. (2012). Assessed traits were crown root-related parameters as follows: the number of connected components (Rccomp); the maximum (MaxR) and median (MedR) number of roots; root system dimensions such as average root width (Rwidth), root network depth (Ndepth), root network length (Nlen) and

root network width (Nwidth); the root density by measuring the network area (NwA), the network surface area (Nsurf) and network volume (Nvol); and the root angle via the network convex area (ConvA). In addition, relative traits presented as ratios such as the ratio of network length to the network volume (specific root length, SRL), the ratio of the maximum root number to the median root number (Network bushiness, Bush), the total network area divided by the network convex area (Network solidity), the lower 2/3 of the root network depth (length distribution, Ldist), and the ratio of the network width to the network depth (network width to depth ratio, NWDR) were also calculated. Root angle (RA) was measured manually using a protractor. Root samples were oven dried afterwards at 60 °C for 72 h, and root dry weight ($RDW_{0–20}$) was determined.

Soil coring was carried out at around mid-grain filling in the INP trial during 2018–2019, 2019–2020 and 2020–2021, in the ILP trial during 2019–2020 and 2020–2021, and in the RLN and RNP trials during 2019–2020 and 2020–2021, respectively. Cores of 100 cm depth were extracted from the centre of each plot using a hydraulic soil corer, then divided into four soil sections (0–25 cm; 20–50 cm; 50–75 cm and 75–100 cm). Approximately 800 g of soil cores were weighed, and from these roots were manually isolated by washing away the soil using tweezers and sieves of different diameters. Once isolated, the roots were saved in a 50 % ethanol. The isolation process took a few months and therefore the sampled cores and roots were kept at low temperatures (−8 °C) temperature at all times. To scan the roots, a 0.1 % methyl violet solution was prepared to dye them for greater contrast. Initially, a 1 g of methyl violet powder was diluted in 100 ml of 100 % ethanol, and then a 1 ml of the concentrated solution was diluted a second time in 9 ml of 100 % ethanol, with the resulting 10 ml solution being further diluted by adding 90 ml of distilled water to give a 0.1 % methyl violet solution. Roots were placed in petri dishes, submerged in the methyl violet solution and kept under dark conditions overnight (Pask et al., 2012). The next day, the dyed roots were carefully dried, scanned (EPSON Perfection 1260, EPSON America Inc., Chicago, USA), and then oven dried at 60 °C for 48 h to determine the root dry weight of each soil section ($RDW_{0–25\ cm}$, $RDW_{25–50\ cm}$, $RDW_{50–75\ cm}$ and $RDW_{75–100\ cm}$). The scanned root images of different soil sections were analysed using the open-source image analysis platform FIJI (Fiji is Just ImageJ; http://fiji.sc/Fiji), to determine root area ($Area_{roots}$) and the coefficient Area/RDW.

2.5. Carbon and nitrogen stable isotope composition and nitrogen content

Analyses were performed in mature grains from all the plots, trials and seasons of the study, and in flag leaves sampled at anthesis during the 2018–2019, 2019–2020 and 2020–2021 seasons. Leaves and grains were dried at 60 °C for a minimum of 48 h and reduced to a fine powder, from which approximately 1 mg was enclosed in tin capsules and analysed using an elemental analyser (Flash 1112 EA; Thermo- Finnigan, Schwerte, Germany) coupled with an isotope ratio mass spectrometer (Delta C IRMS, ThermoFinnigan) operating in continuous flow mode, at the Scientific and Technical facilities of the University of Barcelona. Different secondary standards were used for carbon (IAEA−CH7, IAEA−CH6 and IAEA-600, and USGS 40) and nitrogen (IAEA-600, N1, N2, NO_3, urea and acetanilide) isotope analyses. The nitrogen concentrations (N) in leaves and grains were expressed in percentages (%), and carbon ($\delta^{13}C$) and nitrogen ($\delta^{15}N$) isotope compositions in parts per thousand (‰). The $\delta^{13}C$ and $\delta^{15}N$ results permitted an analytical precision (standard deviation) of 0.1 ‰ and 0.3 ‰, respectively, and were determined following Eq. (2):

$$\delta^{13}C \text{ or } \delta^{15}N\ (‰) = [R_{sample}/R_{standard} - 1] \times 1000 \quad (2)$$

Where $R_{standard}$ is the molar abundance ratio of the secondary standard calibrated against the primary standard Pee Dee Belemnite in the case of carbon ($\delta^{13}C$) and N_2 from air in the case of nitrogen ($\delta^{15}N$) (Farquhar et al., 1989).

Grain nitrogen yield (GNY) was then calculated as:

$$GNY\ (Mg\ ha^{-1}) = (N \text{ concentration in grains x } GY)/100 \quad (3)$$

2.6. Oxygen and hydrogen stable isotope composition

Post anthesis, samples of the stem base (approximately 6–7 cm length) were harvested during two crop seasons (2019–2020 and 2020–2021), from five random plants (main stems) of each selected plot, sealed immediately in analytical tubes and frozen at − 80 °C. Similarly, samples from different soil sections of the cores collected during grain filling (see Section 2.4) were sealed immediately in analytical tubes and kept at − 80 °C. The frozen stems and soil samples were sent for water extraction at the Department of Crop and Forest Sciences, University of Lleida (Spain). Briefly, the first phase (water extraction) was performed using a cryogenic vacuum distillation (CVD) line (Dawson and Ehleringer, 1993). Sample tubes were placed in a heated silicone oil bath (120 °C), and connected with Ultra-TorrTM unions (Swagelok Company, Solon, OH, USA) to a vacuum system (~10 −2 mbar), in series, with U-shaped collector tubes cooled with liquid N_2. Ninety minutes after commencing extraction, the extracted soil water and xylem water in stems was transferred into 2 ml vials and stored at 4 °C until analysis. Afterwards, the oxygen ($\delta^{18}O$) and hydrogen ($\delta^{2}H$) stable isotope compositions of stem water were determined at the Scientific Facilities of University of Lleida (Spain), and the $\delta^{18}O$ and $\delta^{2}H$ of the water soil sections were measured at the Scientific Facilities of the University of Barcelona (Spain). Analyses in both facilities were carried out by isotope-ratio infrared spectroscopy using a Picarro L2120-I isotopic water analyser coupled to an A0211 high-precision vaporiser (Picarro Inc., Sunnyvale, CA, USA). The analytical precision for $\delta^{18}O$ and $\delta^{2}H$ was 0.10‰, and the occurrence of contaminants was tested using Picarro's ChemCorrect post-processing software and corrected, when necessary, following Martín-Gómez et al. (2015). Moreover, CVD was performed at relatively low temperature (120 °C) to preclude the possible presence of a high level of organic contamination (Millar et al., 2018).

The values for $\delta^{18}O$ and $\delta^{2}H$ of the precipitation water throughout the successive seasons (Supplemental Fig. 2) were derived from the monthly predicted values of Valladolid city (few km from the Zamadueñas station) as provided by the "Centro de Estudios y Experimentación de Obras Públicas (CEDEX)" Centro de Estudios y Experimentación de Obras Públicas CEDEX (2022), in collaboration with the Spanish "Agencia Estatal de Meteorología" (https://www.cedex.es/centros-laboratorios/centro-estudios-tecnicas-aplicadas-ceta/lineas-actividad/diseno-metodologia-muestreo-analisis). In addition, $\delta^{18}O$ and $\delta^{2}H$ of precipitation and irrigation water at Zamadueñas Station were collected during anthesis/grain filling for the 2018–2019 (only precipitation) and 2020–2021 (precipitation and irrigation) seasons, and analysed, as above at the facilities of the University of Barcelona.

2.7. Statistical analyses

Analyses of variance (ANOVA) were performed to test the effect of crop seasons, trials, genotypes and soil sections on the studied traits using SPSS software (IBM SPSS Statistics 25, Inc., Chicago, IL; USA). The same software was used (i) to reveal differences within trials and soil sections following the post-hoc Tukey-b test, (ii) to determine Pearson correlations between GY and the rest of the studied traits, and (iii) to perform a stepwise multi-regression analysis with GY as the dependent trait. In addition, Random Forest (RF) multi-regression analysis was performed to predict GY under different trials, and to measure the importance of variables introduced by each fitted model using RStudio 1.2.5 (R Foundation for Statistical Computing, Vienna, Austria). For this, the database was randomly split into a training set (80 %) and a test set

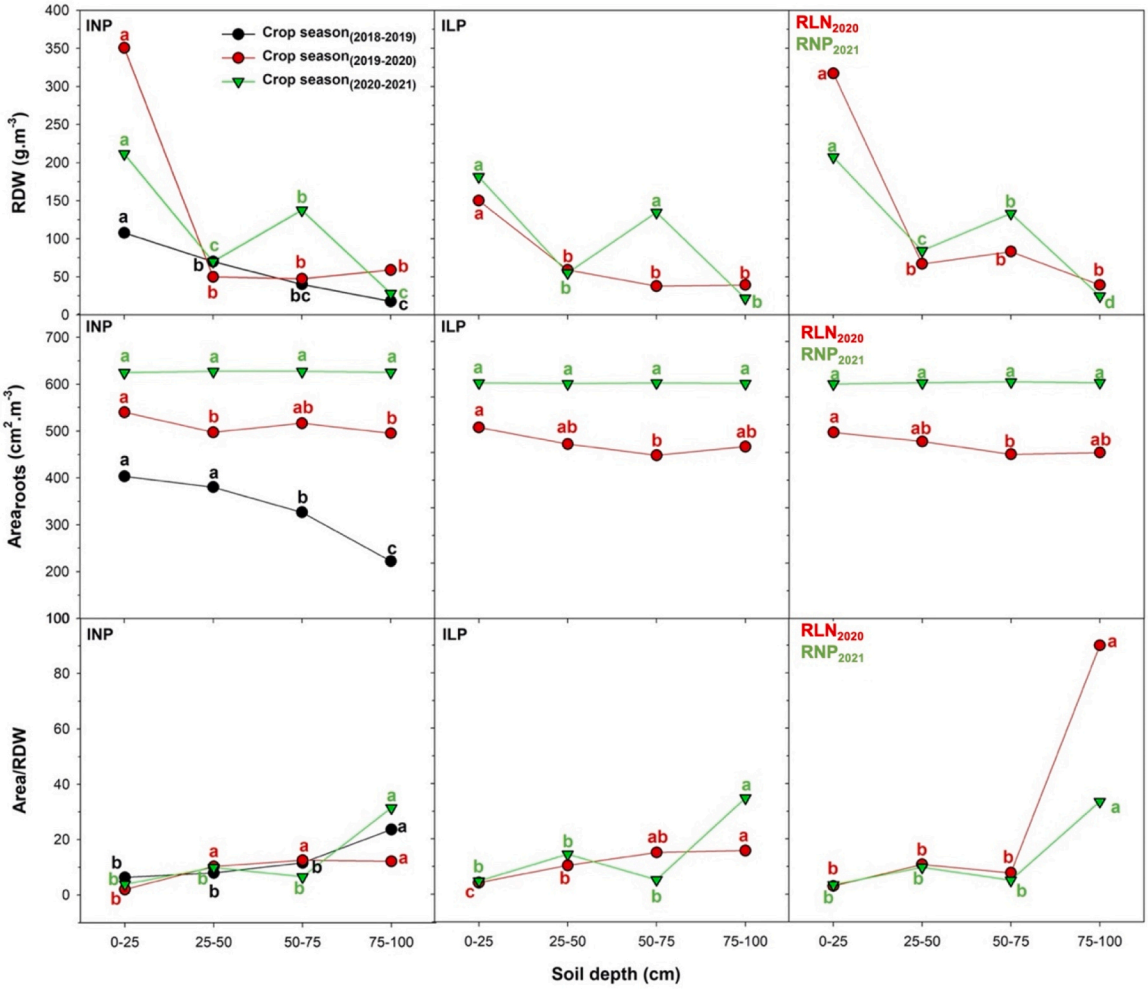

Fig. 2. Average root dry weight (RDW), root area ($Area_{roots}$) and the Area/RDW ratio of selected wheat genotypes grown during different crop seasons (2018–2019; 2019–2020 and 2020–2021) and in trials (INP; ILP; RLN; RNP). Means exhibiting different letters are significantly different ($P < 0.05$) (Tukey-b test) on independent samples for each crop season and within each treatment.

(20 %). For each trial, the model was trained using a resampling in the form of 10 times repeated 10-fold cross-validation, with the final selected models exhibiting the optimum determination coefficient (R^2_{train}) with the lowest root mean square error ($RMSE_{train}$). To evaluate the models' predictive ability on the test set, the R^2_{test} and $RMSE_{test}$ were shown as the Pearson correlation between the tested and the predicted values and the corresponding root mean square error, respectively. Principal component analyses (PCA) were carried out to analyse all the trait categories (including crop growth) in a reduced bi-dimensional platform for each trial using RStudio 1.2.5. Graphs were created using Sigma-plot 10.0 (Systat Software Inc, California; USA).

3. Results

3.1. Season, growth conditions and genotypic effects on crop growth and yield

When the four crop seasons of the study were combined, the effects of season and trial were highly significant on GY, yield components (plant and ear densities, TKW and HI) and crop growth (PH, NDVI and biomass) traits. However, the genotypic effect was only significant for GY and PH (Table 1). The interaction season x trial was significant for all traits except for TKW and plant density, whereas the interaction year x genotype was significant for GY and ear density alone, and the interaction trial x genotype was only significant for GY. The effect of the triple interaction season x trial x genotype was absent on the studied traits. Genotypes across seasons performed best under INP conditions, exhibiting the highest GY, biomass, HI, ear density and PH, as opposed to the RLN conditions where GY overall decreased on average by 35 %. Under ILP and RNP, genotypes showed similar performance in combined seasons (29 % GY decrease compared to INP).

In separate seasons, the trial effect was significant on all traits in each season. However, the genotypic effect was significant only for HI, TKW, plant and ear densities and PH during 2017–2018; for HI and ear number during 2018–2019; for GY, PH and NDVI during 2019–2020; and for GY, TKW, and PH during 2020–2021. The interaction trial x genotype was absent for any of the traits studied during 2017–2018, significant only for biomass during 2018–2019, significant for GY, PH and NDVI during 2019–2020, and significant for GY and PH during 2020–2021 (Table 1). GY, yield components and crop growth traits showed a similar trend in separate seasons as the four seasons were combined, with GY performing the best under INP, and the worst under RLN. The second worst condition was RNP. Differences between irrigation and rainfed trials in grain yield and most of the other traits were maximal during the driest (2018–2019) of the four seasons.

3.2. Season, growth conditions and genotypic effects on crop nitrogen status

To assess crop nitrogen status, the grain nitrogen yield (GNY),

nitrogen concentration (N) and nitrogen isotope composition ($\delta^{15}N$) in leaves and grains were evaluated across seasons and trials (Table 2). When combining seasons, the effects of season and trial were significant on all traits, whereas the effect of genotype was significant on GNY alone. The interaction year x trial was significant for GNY, N_{grain} and $\delta^{15}N_{grain}$, while the tripe interaction year x trial x genotype was only significant for GNY. Overall, GNY was the highest under INP and lower under ILP, RNP and RLN. $\delta^{15}N_{leaf}$ and $\delta^{15}N_{grain}$ were higher under irrigated trials (INP and ILP), and lower under rainfed trials (RNP and RLN).

In separate seasons, the trial effect was significant for GNY and $\delta^{15}N_{grain}$ during the four seasons, for N_{grain} during 2017–2018, 2018–2019 and 2019–2020, for N_{leaf} during 2018–2019, for $\delta^{15}N_{grain}$ during 2017–2018 and for $\delta^{15}N_{leaf}$ during 2018–2019 and 2020–2021. The genotypic effect was significant on GNY during 2018–2019, and on GNY and N_{grain} during 2020–2021. The trial x genotype interaction was significant for GNY during 2020–2021 alone (Table 2). Except for the first season (2017–2018), GNY was higher under INP than in the other treatments, with differences being again maximal during the driest season (2018–2019). Moreover, during 2017–2018, $\delta^{15}N_{grain}$ was higher under RNP and lower under INP and RLN. During 2018–2019, N_{leaf}, $\delta^{15}N_{leaf}$ and $\delta^{15}N_{grain}$ were the highest under irrigated conditions (INP). During 2019–2020, $\delta^{15}N_{grain}$ was the highest under INP, and lower under ILP and RLN. During 2020–2021, $\delta^{15}N_{grain}$ was higher under INP and RNP than under ILP, whereas the opposite occurred for $\delta^{15}N_{leaf}$.

3.3. Season, growth conditions and genotypic effects on crop water status

Crop water status was evaluated through carbon isotope composition ($\delta^{13}C$) in leaves and grains, and canopy temperature depression (CTD) (Table 2). When combining all seasons, the effects of season and trial and the interaction season x trial were significant on CTD and $\delta^{13}C_{grain}$. The genotypic effect was not significant for $\delta^{13}C_{grain}$ and CTD, whereas only the season x genotype interaction was significant for $\delta^{13}C_{grain}$. The effect of the triple interaction was not significant for the assessed traits. Overall, CTD was the highest and $\delta^{13}C_{grain}$ the lowest under irrigated conditions (INP and ILP), as opposed to rainfed conditions (RNP and RLN), where CTD was the lowest and $\delta^{13}C_{grain}$ the highest.

In separate seasons, the trial effect was significant on CTD, $\delta^{13}C_{leaf}$ and $\delta^{13}C_{grain}$ in all seasons, except for $\delta^{13}C_{grain}$ during 2017–2018, and $\delta^{13}C_{leaf}$ during 2020–2021. The genotypic effect was significant for $\delta^{13}C_{grain}$ during all seasons, $\delta^{13}C_{leaf}$ during 2018–2019 and 2019–2020, and CTD during 2019–2020. CTD was higher under INP and RNP and lower under RLN during 2017–2018; during 2018–2019, CTD was higher, and $\delta^{13}C_{leaf}$ and $\delta^{13}C_{grain}$ lower under irrigated (INP) compared with rainfed conditions. During 2019–2020, CTD was higher under ILP than under INP and RLN, whereas $\delta^{13}C_{leaf}$ and $\delta^{13}C_{grain}$ were the lowest under irrigated conditions (INP and ILP), and the highest under RLN. During 2020–2021, both CTD and $\delta^{13}C_{grain}$ were lower under irrigated conditions (INP and ILP) compared with RNP.

3.4. Season, growth conditions and genotype and soil section effects on root characteristics

The structure of the upper part of the root system was assessed through shovelomics. When all seasons considered together, the effects of season, trial, genotype and the interaction season x trial were significant for most shovelomics-derived traits (Supplemental Table 3). Under irrigated conditions (INP and ILP), $RDW_{0–20}$ and root ratios (Bush, Ldist, NWDR and SRL) were lower, and root crown traits (Rccomp, MaxR and MedR), root dimension traits (Rwidth, Ndepth and Nwidth), root density traits (NwA, Nsurf, Nvol) and root angle (ConvA) were higher than under rainfed conditions (RNP and RLN).

In separate seasons, trial and genotypic effects were significant on most root traits during all seasons, except for 2019–2020, where significance was associated mostly with trial effect. During 2017–2018, Rccomp and SRL were higher, and root density ($RDW_{0–20}$, Nwidth, NwA, Nsurf and Nvol) and dimensions (Rwidth, Ndepth and Nlen), root angle (RA and ConvA) and NWDR were lower under INP compared with RNP. As for RLN, $RDW_{0–20}$ and Nwidth, root angle spread (RA) and NWDR were higher. During 2018–2019, most root traits were higher under INP. Root density and dimension were higher under RNP than RLN, whereas Rccomp was higher under RLN than under RNP. During 2019–2020, root number, density, dimension and root angle traits were the highest under ILP conditions, and lower under INP and RLN, except for $RDW_{0–20}$. During the fourth season (2020–2021), root number, root density and dimension, root angle (mainly ConvA) and all root ratios were higher under irrigated conditions (ILP and INP) compared with rainfed conditions (RNP).

Distribution of the root system across the soil profile was assessed through soil coring during the last three seasons and under different growing conditions (Table 3; Fig. 3). The genotypic effect was absent when combining all seasons and in separate seasons. When combining all seasons and treatments, the effects of season, soil section and the season x soil section interaction were significant on the three traits (RDW, $Area_{roots}$ and Area/RDW) assessed (Table 3). However, the effects of trial and the interactions were significant on RDW only (Table 3). RDW was higher under normal planting (INP, RNP and RLN) than at ILP (Fig. 2). Across seasons, the first soil section (0–25 cm) exhibited the highest RDW and $Area_{roots}$ and the lowest Area/RDW, followed by the third soil section (50–75 cm) (Table 3). The fourth soil section (75–100 cm) exhibited the lowest RDW and $Area_{roots}$, and the highest Area/RDW.

RDW, $Area_{roots}$ and Area/RDW in separate seasons varied across soil sections in a rather similar manner as they did when combining seasons. Thus, the effect of soil section was significant on RDW, $Area_{roots}$ and Area/RDW during 2018–2019 and 2019–2020, and on RDW and Area/RDW during 2020–2021, whereas the effect of trial was significant on RDW only and during 2019–2020 (Fig. 2; Table 3).

3.5. Oxygen and hydrogen isotope composition of the soil, plant-stem water and water input

To understand from which soil depth the plants extracted water, the oxygen ($\delta^{18}O$) and hydrogen ($\delta^{2}H$) isotope compositions were evaluated in stem water during 2018–2019 and 2020–2021 (Table 2). In addition, the oxygen ($\delta^{18}O_{soil}$) and hydrogen ($\delta^{2}H_{soil}$) isotope compositions were assessed in different soil sections for the last two seasons (Table 3, Fig. 3), and in the water inputs (precipitation and irrigation) input (Supplemental Fig. 2) were assessed.

The $\delta^{18}O$ and $\delta^{2}H$ of precipitation ($\delta^{18}O_{precipitation}$ and $\delta^{2}H_{precipitation}$) increased from January throughout the crop seasons. Predicted values of $\delta^{18}O_{precipitation}$ and $\delta^{2}H_{precipitation}$ during May, were around − 4.7 ‰ and − 28.8 ‰ for $\delta^{18}O$ and $\delta^{2}H$, respectively (Supplemental Fig. 2). The isotopic values of the irrigation water during 2020–2021 for late May were − 4.5 ‰ and − 35.0 ‰ for $\delta^{18}O$, respectively.

The effect of season was only significant for water $\delta^{2}H_{soil}$, whereas the effects of soil section and trials were significant for both $\delta^{18}O_{soil}$ and $\delta^{2}H_{soil}$ (Table 3). Also, the season x soil section interaction was significant for $\delta^{2}H_{soil}$, and the trial x soil section interaction was significant for $\delta^{18}O_{soil}$ and $\delta^{2}H_{soil}$. Across both seasons, $\delta^{18}O_{soil}$ and $\delta^{2}H_{soil}$ were the highest in the first soil section (0–25 cm), and similar in the rest of the soil sections. In separate seasons, the effects of trial and soil section were significant for $\delta^{18}O_{soil}$ and $\delta^{2}H_{soil}$ during 2019–2020, whereas during 2020–2021, the trial effect was only significant for $\delta^{2}H_{soil}$, and the effect of soil section was significant for $\delta^{18}O_{soil}$ and $\delta^{2}H_{soil}$ (Table 3). Although $\delta^{18}O_{soil}$ and $\delta^{2}H_{soil}$ values in both irrigation trials (INP and ILP) were rather similar and steady across the soil sections, decreases in both $\delta^{18}O_{soil}$ and $\delta^{2}H_{soil}$ across the upper soil sections were steeper under rainfed conditions (RNP, RLP), and they further decreased through the deeper sections in the case of RNP (Fig. 3). On the other hand, the $\delta^{18}O_{soil}$ and $\delta^{2}H_{soil}$ values of RLN (2019–2020) were higher than those of RNP and both irrigation trials (INP, ILP).

Table 2
Effects of crop season (2017-2018; 2018-2019; 2019-2020; 2020-2021), trial (INP, ILP, RNP, RLN), and durum wheat genotypes on nitrogen status traits (grain nitrogen yield (GNY), leaf and grain nitrogen concentrations (N_{leaf} and N_{grain}), nitrogen isotope compositions ($\delta^{15}N_{leaf}$ and $\delta^{15}N_{grain}$)), and water status parameters (canopy temperature depression (CTD), carbon isotope compositions ($\delta^{13}C_{leaf}$ and $\delta^{13}C_{grain}$)) measured in the dry matter of leaves at anthesis and grains at maturity, and oxygen ($\delta^{18}O$) and hydrogen ($\delta^{2}H$) isotope compositions in the water of the stem base at anthesis. ANOVA was tested for trials and genotypes in each crop season and across combined crop seasons.

		Nitrogen status					Water status				
Season	Trial	GNY (Mg ha^{-1})	N_{leaf} (%)	N_{grain} (%)	$\delta^{15}N_{leaf}$ (‰)	$\delta^{15}N_{grain}$ (‰)	CTD (°C)	$\delta^{13}C_{leaf}$ (‰)	$\delta^{13}C_{grain}$ (‰)	$\delta^{18}O_{stem}$ (‰)	$\delta^{2}H_{stem}$ (‰)
2017–2018	INP	0.123ab ± 0.007	-	1.9b± 0.0	-	2.2b± 0.1	0.51a± 0.37	-	-26.6a± 0.1	-6.1 ± 0.2	-57.3 ± 1.0
	RNP	0.130a ± 0.006	-	2.2a± 0.1	-	3.5a± 0.3	1.19a± 0.51	-	-26.5a± 0.1	-5.4 ± 0.4	-58.5 ± 2.0
	RLN	0.101b ± 0.010	-	2.0ab ± 0.1	-	2.3b± 0.2	-1.25b ± 0.41	-	-26.5a± 0.1	-4.2 ± 0.7	-53.5 ± 2.5
	Trial (T)	< 0.050	-	< 0.050	-	< 0.001	< 0.010	-	ns	-	-
	Genotype (G)	ns	-	ns	-	ns	ns	-	< 0.010	-	-
	T xG	ns	-	ns	-	ns	ns	-	ns	-	-
2018–2019	INP	0.173a ± 0.007	4.1a ± 0.1	2.2b± 0.1	3.0a ± 0.1	2.5a± 0.1	-2.71a ± 0.71	-28.3b ± 0.1	-25.4c± 0.2	-6.5c ± 0.2	-55.2b ± 0.8
	RNP	0.086b ± 0.004	4.1a ± 0.3	3.0a± 0.1	0.6c ± 0.1	1.2b± 0.1	-13.40b ± 1.02	-26.3a ± 0.2	-22.6b± 0.3	-5.2b ± 0.2	-57.1b ± 1.1
	RLN	0.071c ± 0.002	3.5b ± 0.1	2.7a± 0.1	1.7b ± 0.2	2.3a± 0.2	-14.36b ± 0.92	-26.0a ± 0.2	-22.4a± 0.2	-3.7a ± 0.3	-51.9a ± 1.0
	Trial (T)	< 0.001	< 0.050	< 0.001	< 0.001	< 0.001	< 0.001	< 0.001	< 0.001	< 0.001	< 0.001
	Genotype (G)	< 0.010	ns	ns	ns	ns	ns	< 0.010	< 0.050	ns	ns
	TxG	ns	ns	ns	ns	ns	ns	ns	ns	ns	ns
2019–2020	INP	0.196a ± 0.006	-	2.3a± 0.0	1.7a ± 0.2	2.5a± 0.1	-2.05b ± 0.25	-29.0b ± 0.2	-26.6b± 0.1	-	-
	ILP	0.122b ± 0.005	-	2.2ab ± 0.1	-	2.0b± 0.1	0.05a± 0.28	-	-26.4ab ± 0.1	-	-
	RLN	0.127b ± 0.007	-	2.1b± 0.1	2.1a ± 0.3	2.0b± 0.1	-1.68b ± 0.31	-28.4a ± 0.2	-26.3a± 0.1	-	-
	Trial (T)	< 0.001	-	< 0.050	ns	< 0.001	< 0.001	< 0.001	< 0.050	-	-
	Genotype (G)	ns	-	< 0.010	< 0.050	ns	< 0.010	< 0.001	< 0.050	-	-
	TxG	ns	-	ns	ns	ns	ns	ns	< 0.010	-	-
2020–2021	INP	0.124a ± 0.003	-	2.0a± 0.1	3.4b ± 0.2	3.5a± 0.1	-0.88b ± 0.62	-28.3a ± 0.4	-26.5b± 0.1	-5.8a ± 0.2	-52.5a ± 0.9
	ILP	0.100b ± 0.005	-	2.1a± 0.1	4.9a ± 0.2	3.0b± 0.1	2.33ab ± 0.66	-28.0a ± 0.2	-26.2b± 0.2	-5.8a ± 0.2	-53.0a ± 1.1
	RNP	0.097b ± 0.004	-	2.2a± 0.1	2.7c ± 0.1	3.4a± 0.1	2.87a± 1.61	-27.4a ± 0.1	-25.0a± 0.1	-6.7a ± 0.1	-60.0b ± 0.7
	Trial (T)	< 0.001	-	ns	< 0.001	< 0.001	< 0.050	ns	< 0.001	ns	< 0.050
	Gen (G)	< 0.010	-	< 0.001	ns	ns	ns	ns	< 0.010	ns	ns
	TxG	< 0.050	-	ns	ns	ns	ns	ns	ns	ns	ns
All seasons	INP	0.157a ± 0.005	-	2.1b± 0.1	2.6b ± 0.1	2.7a± 0.1	-1.34b ± 0.28	-28.6b ± 0.2	-26.3b± 0.1	-6.2b ± 0.1	-54.3a ± 0.6
	ILP	0.112b ± 0.004	-	2.2b± 0.0	4.9a ± 0.2	2.4ab ± 0.1	1.03a± 0.37	-28.0b ± 0.2	-26.3b± 0.1	-5.8b ± 0.2	-53.0a ± 1.1
	RNP	0.105b ± 0.004	-	2.4a± 0.1	1.7c ± 0.2	2.2b± 0.2	-5.36d ± 0.83	-26.9a ± 0.1	-25.2a± 0.2	-5.9b ± 0.2	-58.6b ± 0.7
	RLN	0.102b ± 0.005	-	2.2b± 0.1	1.9c ± 0.2	2.2b± 0.1	-3.08c± 1.08	-27.2a ± 0.2	-25.2a± 0.2	-3.9a ± 0.3	-52.3a ± 1.0
	Season (S)	< 0.001	-	< 0.001	-	< 0.001	< 0.001	-	< 0.001	ns	ns
	Trial (T)	< 0.001	-	< 0.001	-	< 0.010	< 0.001	-	< 0.001	< 0.001	< 0.001
	Genotype (G)	< 0.050	-	ns	-	ns	ns	-	ns	ns	ns
	SxT	< 0.001	-	< 0.050	-	< 0.001	< 0.001	-	< 0.001	ns	ns
	SxG	ns	-	ns	-	ns	ns	-	< 0.010	ns	ns
	TxG	ns	-	ns	-	ns	ns	-	ns	ns	ns
	SxTxG	< 0.050	-	ns	-	ns	ns	-	ns	ns	ns

Values are means of the selected genotypes in each season with the replicates. Levels of significance for the ANOVA: $P < 0.05$, $P < 0.01$ and $P < 0.001$. Means exhibiting different letters a, b and c, are significantly different ($P < 0.05$) according to Student's t-test on independent samples, within each crop season and across combined seasons. INP, irrigated normal planting. ILP, irrigated late planting. RNP, rainfed normal planting. RLN, rainfed low nitrogen. S, crop season. T, trial. G, genotype. Values of δ18Ostem and δ2Hstem during 2017–2018 are given for one replicate only.

Table 3
Effects of crop season (2018–2019; 2019–2020; 2020–2021), trial (INP, ILP, RNP, RLN), genotypes and soil section (0–25 cm; 20–50 cm; 50–75 cm; 75–100 cm) on root dry weight (RDW), root area ($Area_{roots}$) the Area/RDW ratio; and on soil water oxygen ($\delta^{18}O_{soil}$) and hydrogen ($\delta\ ^{2}H_{soil}$) stable isotope compositions.

	Genotype effect						Soil section effect					
		Cores			Soil water			Cores			Soil water	
Season		RDW	$Area_{roots}$	Area/RDW	$\delta^{18}O_{soil}$	$\delta^{2}H_{soil}$		RDW	$Area_{roots}$	Area/RDW	$\delta^{18}O_{soil}$	$\delta^{2}H_{soil}$
2018–2019	Genotype (G)	ns	ns	ns	-	-	Section (Sect)	< 0.001	< 0.001	< 0.001	-	-
2019–2020	Trial (T)	ns	ns	ns	< 0.001	< 0.001	Trial (T)	< 0.010	ns	ns	< 0.001	< 0.001
	Genotype (G)	ns	ns	ns	ns	ns	Section (Sect)	< 0.001	< 0.001	< 0.010	< 0.001	< 0.001
	TxG	ns	ns	ns	ns	ns	TxSect	< 0.010	ns	ns	ns	ns
2020–2021	Trial (T)	ns	ns	ns	ns	< 0.050	Trial (T)	ns	ns	ns	ns	< 0.050
	Genotype (G)	ns	ns	ns	ns	ns	Section (Sect)	< 0.001	ns	< 0.001	< 0.001	< 0.010
	TxG	ns	ns	ns	ns	ns	TxSect	ns	ns	ns	< 0.001	< 0.050
All seasons	INP	95.4	484.2	45.5a	-6.4a	-54.4bc	0–25	210.4a	559.9a	20.6c	-5.5a	-48.7a
	ILP	98.2	577.4	72.2a	-6.2b	-52.0b	25–50	67.3c	545.0b	55.6b	-6.1b	-53.7b
	RNP	118.9	625.2	107.1	-6.4b	-56.6c	50–75	92.9b	535.2b	31.9bc	-6.3b	-54.3b
	RLN	126.6	512.9	27.8	-4.6a	-43.4a	75–100	36.3d	494.8c	151.7a	-6.5b	-54.6b
	Season (S)	< 0.050	< 0.001	< 0.010	ns	ns	Season (S)	< 0.001	< 0.001	< 0.001	ns	< 0.001
	Trial (T)	ns	ns	ns	< 0.001	< 0.001	Trial (T)	< 0.010	ns	ns	< 0.001	< 0.001
	Genotype (G)	ns	ns	ns	ns	ns	Section (Sect)	< 0.001	< 0.001	< 0.001	< 0.001	< 0.001
	SxT	ns	ns	ns	ns	ns	SxT	< 0.050	ns	ns	ns	ns
	SxG	ns	< 0.010	ns	ns	ns	SxSect	< 0.001	< 0.001	< 0.001	ns	< 0.001
	TxG	ns	ns	ns	ns	ns	TxSect	< 0.001	ns	ns	< 0.001	< 0.010
	SxTxG	ns	ns	ns	ns	ns	SxTxSect	< 0.010	ns	ns	ns	ns

Values are means of the selected genotypes in each season with three replicates. Levels of significance for the ANOVA: $P < 0.05$, $P < 0.01$ and $P < 0.001$. Means exhibiting different letters a, b and c, are significantly different ($P < 0.05$) according to Student's t-test on independent samples, within each crop season and across combined seasons. INP, irrigated normal planting. ILP, irrigated late planting. RNP, rainfed normal planting. RLN, rainfed low nitrogen. S, crop season. T, trial. G, genotype. Sect, soil section. Trials tested were INP during 2018–2019; INP, ILP and RLN during 2019–2020; and INP, ILP and RNP during 2020–2021.

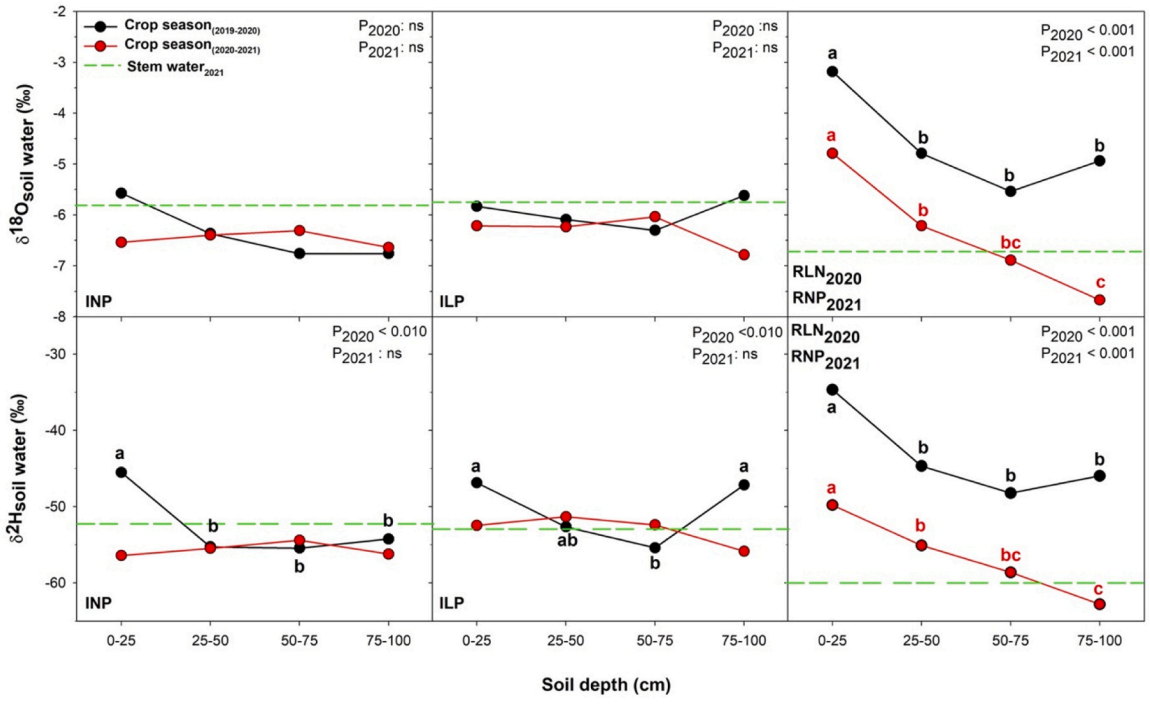

Fig. 3. Average values of soil water oxygen ($\delta^{18}O$) and hydrogen ($\delta^{2}H$) stable isotope compositions sampled in different soil sections (0–25 cm; 20–50 cm; 50–75 cm and 75–100 cm), during the crop seasons 2019–2020 and 2020–2021. Means exhibiting different letters are significantly different ($P < 0.05$) (Tukey-b test) on independent samples for each crop season and within each treatment. The baselines represent the mean values of oxygen ($\delta^{18}O$) and hydrogen ($\delta^{2}H$) stable isotope compositions sampled in irrigation water and precipitation during soil sampling.

In stem water, when combining both seasons, only the effect of trial was significant on $\delta^{18}O_{stem}$ and $\delta^{2}H_{stem}$ (Table 2). Thus, the treatment with the lowest values was INP, followed by both ILP and RNP, while RLN exhibited the highest values. Likewise, in separate seasons, only the trial effect was significant for $\delta^{18}O_{stem}$ and $\delta^{2}H_{stem}$ during 2018–2019, and on $\delta^{2}H_{stem}$ during 2020–2021.

3.6. Relationships between grain yield and the studied traits

Pearson correlations of GY against agronomic and crop growth traits, and nitrogen and water status indicators were determined under combined and separated seasons and trials (Supplemental Tables 2 and 3). When combining all cases (seasons and trials), GY was positively

correlated with all agronomic yield components and crop growth traits, together with CTD, and $\delta^{15}N_{grain}$, and negatively correlated with N_{grain} and most of the of stable isotopes ($\delta^{15}N_{leaf}$, $\delta^{13}C_{leaf}$ and $\delta^{13}C_{grain}$, and $\delta^{18}O_{stem}$). Across all seasons and for irrigated trials, biomass, plant and ear densities and PH, and N_{grain} were positively correlated with GY, whereas $\delta^{15}N_{leaf}$, $\delta^{18}O_{stem}$ and $\delta^{2}H_{stem}$ were correlated negatively with GY under INP, and only PH was positively correlated with GY under ILP. For the rainfed trials across all seasons, GY was correlated positively with most agronomic traits and CTD, and negatively with N_{grain}, $\delta^{15}N_{leaf}$, $^{15}N_{grain}$ $\delta^{13}C_{leaf}$ and $\delta^{13}C_{grain}$ under RLN and RNP (Supplemental Table 5). In separate seasons, similar correlation trends were observed of GY, crop growth traits and water status in each season, mainly during 2017–2018 and 2018–2019. In addition, GY correlated with nitrogen status traits mainly under 2018–2019 for combined trials, as well as within RNP (Supplemental Table 5).

Further, Pearson correlations between GY and root traits were evaluated combining all seasons and trials (Supplemental Tables 4 and 5)). Thus, most shovelomic traits were correlated positively with GY, whereas in soil coring-derived traits, $RDW_{50–75\ cm}$ were correlated negatively, and $RDW_{75–100\ cm}$ positively with GY. The $Area_{roots}$ of all soil sections were correlated negatively with GY, while the ratio Area/RDW correlated negatively with GY in three soil sections (0–25 cm, 25–50 cm and 75–100 cm), and positively in the 50–75 cm soil section. In separate trials and combined seasons (Supplemental Table 6), GY correlations were negative with $RDW_{0–20}$, Rwidth and network solidity under INP; positive with MaxR, MedR, Nwidth, RA, NWDR and SRL, and negative with Rwidth and Ldist under ILP; positive under MaxR, MedR, Nlen, Nwidth, ConvA and SRL, and negative with Rwidth under RLN; and positive with $RDW_{0–20}$, RA and Ldist, and negative with Rccomp under RNP.

In separate seasons and combined trials (Supplemental Table 7), GY correlations were mostly shown with shovelomic-derived traits during 2018–2019 and 2020–2021. In separate seasons and separate trials, positive correlations were shown during 2018–2019 between GY and root crown, density, dimension, root angle and Ldist under INP; and with density and dimensions under RLN and RNP. During 2019–2020, GY was correlated positively with root crown, density, dimension and root angle under RLN; and with RA and NWDR under ILP.

3.7. Relationships of $\delta^{18}O_{stem}$ and $\delta^{2}H_{stem}$ with water and nitrogen status and root traits

Besides the correlation of $\delta^{18}O_{stem}$ with GY (and to a lesser extent of $\delta^{2}H_{stem}$ with GY) of both rainfed and support irrigation normal planting trials (Fig. 4), $\delta^{18}O_{stem}$ was also negatively correlated with the CTD of the rainfed trials, as well as with both categories (normal planting rainfed and irrigation) of the combined trials. Moreover, $\delta^{18}O_{stem}$ was positively correlated with $\delta^{13}C$ of mature grains from the rainfed trials, and negatively with the $\delta^{15}N$ of mature grains from the rainfed trials, as well as combining both categories (rainfed and support irrigation) (Fig. 4). Furthermore, in the case of the two support-irrigation categories of trials (INP and ILP), $\delta^{18}O_{stem}$ was positively correlated with the total digital (i.e. pixel) root area of the two deeper (50–100 cm) core sections, and negatively correlated with the $Area/RDW_{50–75\ cm}$. $\delta^{2}H_{stem}$ followed the same pattern but in general the relationships were weaker. $\delta^{18}O_{stem}$ and $\delta^{12}H_{stem}$ were also correlated with some shovelomic traits, but in this case only in the INP trial. Thus, the root-dimensional trait R_{width} together with the root angle RA were correlated positively with $\delta^{18}O_{stem}$ and $\delta^{2}H_{stem}$, while the ratios Ldist and $SRL_{0–20\ cm}$, were correlated negatively. Under rainfed conditions the relationships between root characteristics and $\delta^{18}O_{stem}$ and $\delta^{2}H_{stem}$ were scarcer, the shovelomics Ldist ratio was corelated negatively with $\delta^{2}H_{stem}$. However, unlike the support irrigation trials, $Area_{roots\ 50–75\ cm}$ was negatively correlated with $\delta^{18}O_{stem}$ (Supplemental Table 8).

3.8. GY-prediction models

Multilinear regression analyses were carried out to evaluate the contribution of nitrogen and water status traits, together with root traits to explain GY performance across seasons and under combined and separated trials (Table 4), and under separated seasons and trials (Supplemental Table 10). Given their direct relationship to GY, all the agronomic yield components and growth traits were excluded from the prediction models. When combining all seasons and trials, regression models explained 47.6 % of GY variability with $\delta^{13}C_{grain}$ and $RDW_{0–20}$ as negative explicative variables, and MaxR and $\delta^{15}N_{grain}$ as positive explicative variables. Across seasons and under INP, 44.6 % of GY variability was explained using $RDW_{0–20}$, $RA_{0–20}$ and network solidity as

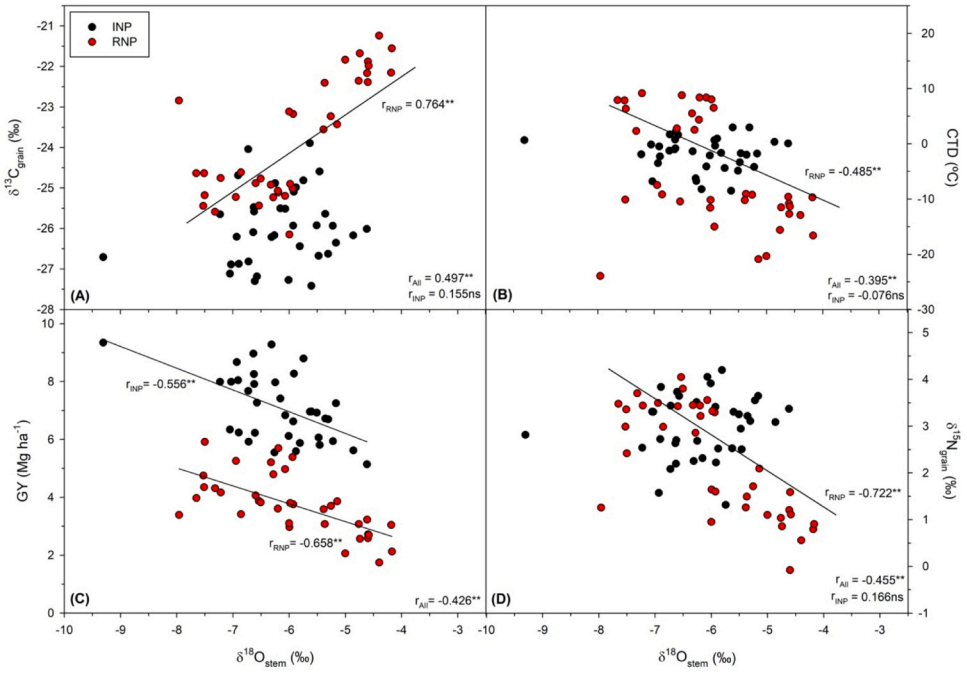

Fig. 4. Relationship between the oxygen isotope composition of the water in the base of the stem ($\delta^{18}O_{stem}$) and the carbon isotope composition ($\delta^{13}C$) of mature grains (A), the canopy temperature depression (CTD) measured during grain filling (B), grain yield (GY) (C), and the nitrogen isotope composition ($\delta^{15}N$) of mature grains (D). Each symbol represents an individual plot value of a rainfed (open symbols) or a support irrigation (filled symbols) trial, under normal planting (INP and RNP, respectively) from the 2018–2019 and 2020–2021 growing seasons.

Table 4
Multi-linear regression (stepwise) of grain yield (GY) as the dependent variable, and canopy temperature depression (CTD), stable carbon and nitrogen isotope compositions ($\delta^{13}C$ and $\delta^{15}N$) and nitrogen concentration (N) of mature grains, and shovelomic root traits as independent variables. For each stepwise equation, the fitted model was significant ($P < 0.001$) with (1.2 <Durbin-Watson< 2) and collinearity was within the acceptable range (VIF<10). R^2 displays the reliability of the fitted regression line to the data used in the stepwise regression ($R^2_{stepwise}$), and random forest regression (R^2_{Train} and R^2_{Test}). Standard error of the dependent variable was given for the stepwise regression as (SE), and for random forest regression as RMSE of the training set ($RMSE_{Train}$) and the test set ($RMSE_{Test}$).

	Stepwise			Random Forest			
Model	Equation	R^2	SE	R^2_{Train}	$RMSE_{Train}$	R^2_{Test}	$RMSE_{Test}$
All	$GY = -13.07 - 0.57 * \delta^{13}C_{grain} - 0.29 * RDW_{0-20} + 0.25 * MaxR + 0.16 * \delta^{15}N_{grain}$	0.476	1.3	0.478	1.8	0.590	1.3
INP	$GY = 11.85 - 0.69 * RDW_{0-20} + 0.34 * Nlen - 0.26 * RA - 0.23 * Network\ solidity$	0.446	1.0	0.225	1.3	0.344	1.3
ILP	$GY = 2.03 + 0.69 * RA + 0.26 * CTD$	0.397	0.6	0.020	0.6	0.340	0.6
RLN	$GY = -23.78 - 1.02 * \delta^{13}C_{grain} + 0.48 * Rcomp + 0.21 * \delta^{15}N_{grain}$	0.663	1.1	0.522	1.7	0.820	1.0
RNP	$GY = -10.63 - 0.76 * \delta^{13}C_{grain} + 0.22 * Ldist$	0.774	0.7	0.696	0.5	0.727	0.9

Regressions were generated using individual plots of the selected genotypes across all crop seasons. To generate stepwise and random forest regression models, 234 plots were used for All, 78 plots for INP, 42 plots for ILP, 60 plots for RLN and 54 plots for RNP.

negative traits, and Nlen as a positive trait; under ILP, 39.7 % of GY was explained with RA_{0-20} and CTD as positive traits; under RLN, 66.3 % of GY variability was explained using $\delta^{13}C_{grain}$ as a negative trait, and Rccomp and $\delta^{15}N_{grain}$ as positive traits; and finally under RNP, 77.4 % of GY variability was explained using $\delta^{13}C_{grain}$ as a negative trait and Ldist as a positive trait (Table 4). Similar results were achieved when performing analysis using Random Forest (RF) models (Supplemental Table 9). Furthermore, similar explanatory traits were given by the RF regression model to the stepwise model when combining all seasons and trials, and in combined seasons and separate trials (Table 4). When separating seasons and combining trials, GY performance was explained as the best during 2018–2019 ($R^2_{stepwise} = 90.8$ %; $R^2_{RF} = 82.9$ %), by introducing $\delta^{13}C_{grain}$, $\delta^{18}O_{stem}$ and Nwidth as negative explicative variables, and Nlen, Ldist and $\delta^{2}H_{stem}$ as positive explanatory variables in the stepwise model (Supplemental Table 8). Similar traits were introduced in the RF model as well (Supplemental Table 11).

Additionally, principal components analyses were carried out to assess further relationships between all studied traits in a bi-dimensional platform for each growing condition across seasons (Fig. 5) and in separate seasons (Supplemental Fig. 1). Across seasons, the two principal components explained 53.5 % of the variability under INP, with N_{grain}, RA, Rccomp and SRL traits positioned in the same direction as GY, and RDW, $\delta^{15}N_{grain}$ and Rwidth in the opposite direction from GY. In a similar manner, 60.8 % of the variability was explained under ILP, with N_{grain}, PH, Rccomp, RA and SRL positioned in the same direction as GY, and $\delta^{13}C_{grain}$, $\delta^{15}N_{grain}$ and Rwidth in the opposite direction. Regarding the two rainfed conditions, the results were very similar. Thus, under RLN 69.4 % of the variability was explained, with PH, CTD, SRL and Rccomp traits placed in the same direction as GY, and N_{grain}, $\delta^{13}C_{grain}$, $\delta^{15}N_{grain}$ and Rwidth in the opposite direction. Under RNP, 69.3 % of the variability was explained, with PH, NDVI, $\delta^{15}N_{grain}$, CTD, RA and RDW placed in the same direction with GY, and $\delta^{13}C_{grain}$, Rccomp, N_{grain} and Rwidth in the opposite direction to GY (Fig. 5).

In separate seasons, the variability explained under INP trials ranged from 39.1 % (2019–2020) to 52.8 % (2017–2018), with CTD and RDW_{0-20} being positive traits with GY during the three consecutive seasons (2017–208; 2018–2019 and 2019–2020), $\delta^{18}O_{stem}$ and $\delta^{2}H_{stem}$ being negative traits during 2018–2019 and 2020–2021, and $\delta^{13}C_{grain}$ being a negative trait in all seasons. Under ILP, the explained variabilities were 45.5% during 2019–2020 and 48.8 % during 2020–2021, with RDW_{0-20}, Rccomp and $\delta^{15}N_{grain}$ being positive traits, and $\delta^{13}C_{grain}$ being a negative trait relative to GY during both seasons, RA being a positive trait relative to GY under 2019–2020, and $\delta^{18}O_{stem}$ and $\delta^{2}H_{stem}$ being negative traits relative to GY during 2020–2021. Under RLN, the explained variabilities were 55.3 %, 49.9 % and 51.3 % during 2017–2018, 2018–2019 and 2020–2021, respectively. For the three seasons, CTD, RDW_{0-20}, $\delta^{15}N_{grain}$ were positive traits relative to GY, and $\delta^{13}C_{grain}$ was a negative trait to GY. Moreover, RA was placed in the same direction as GY during 2020–2021, and oppositely to GY during 2017–2018 and 2018–2019, together with $\delta^{18}O_{stem}$ and $\delta^{2}H_{stem}$. Under RNP, variabilities of 50.3 %, 48.5 % and 41.3 % were explained during 2017–2018, 2018–2019 and 2019–2020, respectively. For each of the three seasons, Rwidth, PH and NDVI were positive traits relative to GY, and RDW_{0-20}, RA and $\delta^{13}C_{grain}$ were negative traits to GY. $\delta^{18}O_{stem}$ and $\delta^{2}H_{stem}$ were negative traits during 2018–2019, as were RA and SRL during 2018–17–2018 and 2018–2019 (Supplemental Fig. 2).

4. Discussion

4.1. Environmental and genotypic effects on crop growth and yield performance

The field experiments included in this study covered a broad environmental range of effects on durum wheat growth and yield performance. The comparative effects of season, trial and genotypes were assessed through the percentage of the sum of squares (SS) on GY.

Season (SS_{season}= 13.70 % of SS_{model}) and crop management (SS_{trial} = 48.7 % of SS_{model}) were major factors in the study and accounted for a wide range of grain yields under different Mediterranean scenarios. By contrast, the genotypic effect, even if significant, was minor on GY ($SS_{genotype}$ = 2.97 % of SS_{model}), which agrees with previous studies highlighting the reduced genotypic variation in durum wheat compared with bread wheat (Asins and Carbonell, 1989; Martínez-Moreno et al., 2020). Similarly, the genotypic effect was significant, albeit minor, on water and nitrogen status and most shovelomics-derived traits and was absent from soil-coring root traits. The lack of genotypic differences for the soil coring root traits in our study was likely due to different factors, which may offset minor differences related to genotypic variability (Hodgkinson et al., 2017; Wasson et al., 2014). Among these factors was the low accuracy or the relatively high error in the methodology for root assessment, but also because of the strong plasticity of roots in response to specific growing conditions (Bai et al., 2019; Paez-Garcia et al., 2015; Wasaya et al., 2018). Furthermore, the season and trial effects were highly significant, not only for the growth, water and nitrogen physiological parameters, but also for most of the root traits studied, which make them amenable characterisation during yield performance studies under different crop management conditions or for a given growth conditions across seasons. Moreover, since most of the root characteristics studied have shown genotypic differences, they were amenable for defining wheat ideotypes under specific management practices and seasons.

4.2. GY-prediction models and root traits

The importance of traits that inform about root architecture mostly relies on the interplay between root distribution, root function, and their effect on crop productivity, as well as the availability of water and nutrients in the soil (Chen et al., 2017). Root architecture is also characterised by a wide phenotypic plasticity (Clark et al., 2011; Hodge, 2009; Malamy, 2005). Therefore, it is advisable to study the contribution of root traits under different settings, including environmental growing conditions such as combinations of managements methods across seasons (i) and within a season (ii), as well as in a given crop management condition across seasons (iii) and within a season (iv). We addressed these factors through GY-prediction models that included, alongside traits reporting on the water and nitrogen status of the crop, root characteristics (Boudiar et al., 2021; Manschadi et al., 2010; Nehe et al., 2021; Thoday-Kennedy et al., 2022).

For the first three scenarios we ran stepwise and random forest (RF) models, complemented with PCA, while for the fourth setting, given the limited size of the data set, RF was not run. Some season-specific models also included stable oxygen and hydrogen signatures of the stem water. Similarly, the PCA analyses included crop growth traits, while these traits were omitted in the multilinear stepwise and RF analyses.

The strength of the predicting models was good overall. When combining all seasons and agronomic conditions, stepwise and RF models explained nearly 50 % of the variability in GY. Within each season, prediction models that combined all the growing conditions were highly variable in their performance. The rather variable performance of the prediction models was related to the range of GY variability, which was the highest in the driest season and the lowest in the wet season. This illustrates the need for a wide range of values in the data set to develop strong GY prediction models when combining very diverse agronomic conditions, including different irrigation, fertilisation and planting date designs (Barraclough et al., 1989; Chapman et al., 2012; Hernandez-Ochoa et al., 2019). By contrast, models for each growing condition alone, across seasons, were more stable, explaining between 40 % and 80 % of the variability in GY, particularly when using stepwise models.

4.3. Crop performance and root traits across agronomic conditions

When combining all seasons and growth conditions, GY prediction provided by stepwise and RF models integrated water status traits (CTD

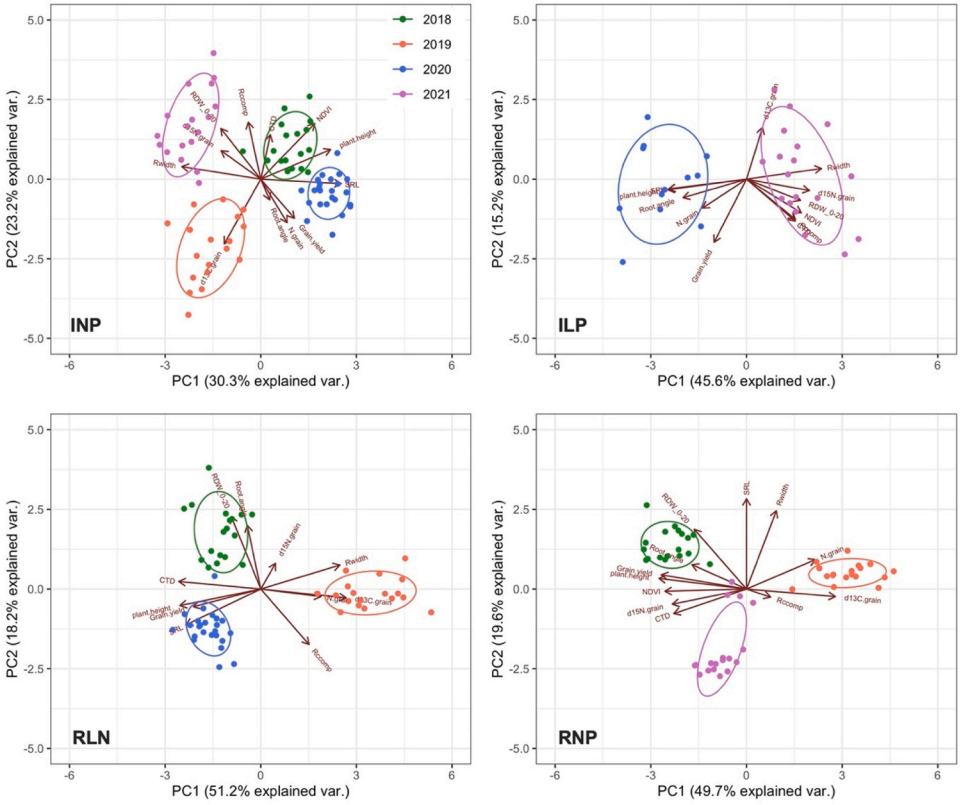

Fig. 5. Principal component analysis (PCA) of the selected wheat cultivars grown during four consecutive crop seasons (2017–2018; 2018–2019; 2019–2020 and 2020–2021) combined, and under different treatments (INP, ILP, RLN and RNP). The variables included in the analysis are grain yield, plant height, NDVI, canopy temperature depression (CTD), nitrogen concentration (N_{grain}) of grain dry matter, stable carbon ($\delta^{13}C_{grain}$) and nitrogen ($\delta^{15}N_{grain}$) compositions of grain dry matter, oxygen ($\delta^{18}O_{stem}$) and hydrogen ($\delta^{2}H_{stem}$) isotope compositions of the stem water, and selected root traits: root dry weight in the 0–20 cm soil layer (RDW_{0-20}), average root width (Rwidth), number of connected components in the root crown (Rccomp), specific root length (SRL_{0-20}), and root angle measured with a protractor (Root angle).

and/or $\delta^{13}C_{grain}$) as primary explicative variables, which indicates that water status was the main driver of GY variability when considering the overall effect of season x growth conditions. CTD and $\delta^{13}C$ have been used as time instantaneous (CTD) and integrative ($\delta^{13}C$) indicators of the effect of water stress on yield (Araus and Cairns, 2014). Cooler canopies, as shown by higher CTD values, have been linked to deeper roots (Lopes and Reynolds, 2010; Reynolds et al., 2007; Wasaya et al., 2018), and higher CTD and lower $\delta^{13}C$ values are often related to higher grain yield performance in wheat genotypes (Araus et al., 2003, 2008; Blum, 2009; Chairi et al., 2020; Farquhar et al., 1989; Rezzouk et al., 2020, 2022). Crown root traits informing about root density ($RDW_{0–20}$) and number (MaxR) in the upper part of the soil (Fradgley et al., 2020; He et al., 2022; York et al., 2018a) were the second most relevant variables to integrate into the GY prediction model.

When considering seasons separately but combining all the growing conditions assayed in a season, the main trait introduced by the model was also informing about better water status (lower $\delta^{13}C$ or higher CTD). This agrees with water conditions being the main factor affecting wheat productivity across Mediterranean environments (Araus et al., 2014; Rezzouk et al., 2022). In addition, for the most robust model, which corresponded to the driest season (2018–2019), root traits informing about deep rooting tendencies, such as greater root length (Nlen and Ldist) in the upper soil (Armengaud, 2009; Clark et al., 2011; He et al., 2022; Iyer-Pascuzzi et al., 2010) and root system spread such as a lower Nwidth (Clark et al., 2011; Iyer-Pascuzzi et al., 2010) were also involved. Moreover, $\delta^{18}O$ and $\delta^{2}H$ of the stem water, which in principle inform about the soil depth from which water is extracted (Kale Çelik et al., 2018; Sanchez-Bragado et al., 2019; Rezzouk et al., 2022) were also included.

4.4. Crop performance within agronomic conditions

Except for support irrigation and normal planting conditions, the specific models for each growing condition throughout the four seasons also included better water status (lower $\delta^{13}C$ or higher CTD) as the first chosen trait in the models for rainfed conditions. In the case of RLN, a better nitrogen status (higher $\delta^{15}N$) was also included in the model. These results again stress that the variability in precipitation/evapotranspiration is an important factor affecting wheat productivity under Mediterranean conditions, particularly (but not only) under rainfed conditions (Araus and Slafer, 2011; Rezzouk et al., 2022). Besides that, all four growth conditions-specific models included shovelomic-assessed root traits. In the case of support irrigation conditions, root angle spread had a clear role, with steeper roots (lower RA) being fundamental during INP, while shallower roots (higher RA) were involved in the ILP conditions. Moreover, lower root mass dry weight (lower $RDW_{0–20}$ and Network solidity) but a greater root length (greater Nlen) in the topsoil were introduced into the INP model. The shallow root system of ILP is coherent with the fact that Mediterranean conditions are characterised by a progressive decrease in precipitation together with an increase in evapotranspiration during late spring, which makes irrigation the main source of water. In the case of INP, a root system that is more evenly distributed (keeping greater root length in the topsoil alongside with steeper roots) across the soil profile represents a more efficient alternative. Such a dichotomy in the root system associated with the planting date has been reported before (Bai et al., 2019; Rezzouk et al., 2022).

The rainfed conditions included a denser root system in the topsoil as a positive trait; specifically, a greater root ramification (greater Rccomp) in the case of RLN, and a greater network length distribution (larger Ldist) under RNP. This root architecture may contribute to a more efficient capture of effective water by the crop, particularly under low and erratic precipitation conditions. A developed root system in the topsoil has been reported to be an adaptation strategy to tackle Mediterranean conditions (Condon, 2020; Passioura, 1983; Rezzouk et al., 2022). Nevertheless, this conclusion does not preclude the presence of a well-developed root architecture down the soil profile (Barraclough et al., 1989).

The PCA added further information on the traits involved in crop performance within a given agronomic conditions across seasons. Under RNP conditions, the best yielding genotypes were associated with stronger aerial growth (higher PH and NDVI), better water (higher CTD and lower $\delta^{13}C$) and nitrogen status (higher $\delta^{15}N$), together with shallower root angle (higher RA), and related to this a somewhat greater root density (higher $RDW_{0–20}$ but lower Rccomp) in the topsoil. Under RLN, crops with higher GY were associated again with stronger aerial growth (greater PH) together with a better water status (higher CTD and lower $\delta^{13}C$), while the root system was characterised by thinner roots (higher SRL and lower Rwidth) in the topsoil. However, root angle and root density were not involved, suggesting that the lack of nitrogen prevented roots from properly exploring the soil profile. Higher root density together with thinner roots are considered positive root traits contributing to water and nutrient uptake (Kong et al., 2014; Paez-Garcia et al., 2015; Robbins and Dinneny, 2015; Sun et al., 2015; Tian et al., 2014). Under INP, GY was not clearly associated with a stronger growth or a better water or nitrogen status, but to some extent a shallower root angle (higher RA but close to the centroid of the PCA), lower root density (lower $RDW_{0–20}$ and Rccomp) and thinner roots (higher SRL and lower Rwidth) in the topsoil. Under ILP, highly productive crops were again not clearly associated with greater growth, but exhibited better water status (lower $\delta^{13}C$), shallower root angle (higher RA) and thinner roots (higher SRL and lower Rwidth). The lack of a clear association of grain yield with growth and green biomass under irrigation conditions may be due, at least in fact, to the saturation of NDVI above values of 0.5 (Aparicio et al., 2000; Cabrera-Bosquet et al., 2011) and a minor effect of moderate/mild heat stress on plant height. However, rainfed conditions, and to a lesser extent the lack of N fertilisation, placed NDVI values in a linear relationship with green biomass and grain yield (Marti et al., 2007; Cabrera-Bosquet et al., 2011). Moreover, plant height has proven to be a good indicator of the effect of severe water stress on crop growth and yield (Khaliq et al., 2004; Akram et al., 2008).

4.5. Genotypic performance within a given agronomic condition and season

In order to explore genotypic performance, PCA and multilinear stepwise analyses were run for each of the trials and seasons. This included for some seasons the isotope signatures of the stem water as additional traits. Concerning PCA, when evaluating INP in separate seasons, high yielding genotypes exhibited greater growth in general (higher PH and/or NDVI) and better water status (lower $\delta^{13}C$ and/or higher CTD), together with steeper root angle (lower RA). The association between deep rooting and a more vertical and greater seminal root wheat was reported previously in high yielding cultivars (Bai et al., 2019; Wasaya et al., 2018). In addition, in the two seasons where stem water was analysed, both $\delta^{18}O$ and $\delta^{2}H$ were positioned opposite to GY, suggesting the most productive genotypes extracted water deeper from the soil profile (Martín-Gómez et al., 2015; Rezzouk et al., 2022; Wang et al., 2010). These results support the concept that deeper root systems may confer genotypic adaptation under the mild to moderate water stress conditions experienced under support irrigation (Hodge, 2009; Li et al., 2019; Malamy, 2005; Vadez, 2014). Moreover, the stepwise analysis for 2018–2019 also supports a greater root density (greater Nsurf, Rccomp and Ldist) in the topsoil for the driest season. Overall, these results evidence a dual (shallow and deeper) soil system.

Under ILP, the best yielding genotypes again exhibited stronger plant growth (higher PH), and better water status (lower $\delta^{13}C$ and/or higher CTD), but also better nitrogen (higher $\delta^{15}N$) status, together with more superficial rooting, as shown by wider angle spread (higher RA), but also access in depth of water as shown by thinner roots (higher SRL and lower Rwidth) and deeper water uptake (lower $\delta^{18}O$ and $\delta^{2}H$ of stem water). These results suggest that even if shallow, rooting is an obvious adaptation to late planting under irrigation conditions, ensuring that access

to water at deeper soil profiles may be of value. Setting canopy cooling mechanisms such as deep rooting and superficial root growth, is a common response of wheat plants as a coping mechanism to elevated temperatures when under irrigation conditions (Pinto and Reynolds, 2015; Rezzouk et al., 2022). In addition, a better nitrogen status can reflect a greater stay green status in genotypes, which maintain greener canopies through an active photosynthesis rate (Joshi et al., 2007; York et al., 2018b), and it promotes the development of deeper roots in wheat genotypes under drought stress (Christopher et al., 2008).

Under RNP, high yielding genotypes were correlated positively with stronger growth (higher NDVI and/or PH) and better water status (lower $\delta^{13}C$ and higher CTD). Moreover, the best yielding genotypes also exhibited less superficial root growth with lower root density (lower RDW_{0-20}), together with steeper root angle growth (lower RA) and lower $\delta^{18}O$ and $\delta^{2}H$ of the stem water. In addition, the stepwise analysis also supported more vertical growth (greater Ndepth), at least for the driest season (2018–2019). A root system prioritising deeper roots may be able to take advantage of strong but scarce rainfall and optimise the capture of water at depth (Wasson et al., 2012).

Likewise, genotypes with the highest yield under RLN conditions were also associated with higher crop growth and better water status (lower $\delta^{13}C$ and/or higher CTD) and with better nitrogen status (higher $\delta^{15}N_{grain}$). The higher $\delta^{15}N$ associated with high yielding genotypes may be the due to a direct physiological effect on the nitrogen metabolism associated with a better water status (Yousfi et al., 2009, 2012) or because of a higher soil nitrogen uptake by the plant (Rezzouk et al., 2022; Sanchez-Bragado et al., 2017; Serret et al., 2008; Yousfi et al., 2009) or both. In the last case, the crop not only uses nitrogen derived from chemical fertilisers (with a $\delta^{15}N$ close to 0 ‰) but also derives nitrogen from nitrification of the organic matter already present in the soil (which has markedly higher $\delta^{15}N$). Moreover, the best yielding genotypes under RLN exhibited somewhat higher crown root density (higher RDW_{0-20} and/or higher Rccomp) together with steeper root angle (lower RA). A higher root density (higher MedR) and weight (higher RDW) in topsoil was also evidenced through stepwise analysis, at least during the 2019–2020 season. A dual root system comprising shallow roots and others at depth may allow the plant to take advantage of low precipitation as well as a lack of nitrogen, optimising the capture of resources (water and nitrogen) at different depths in the soil (Wasson et al., 2012) and therefore increasing the effective use of water (Blum, 2009) and mineral resources. In that sense, Trachsel et al. (2013) reported for maize that genotypes form shallow roots when grown under well nitrogen fertilised environments, and steeper roots that grow at depth when under low nitrogen fertilisation conditions.

4.6. *Exploring root architecture at depth: soil coring traits and $\delta^{18}O$ and $\delta^{2}H$ of stem water as phenotyping traits*

The high plasticity of the root system may explain why the pattern of root traits conferring adaptation may differ among growing conditions and seasons. The shovelomics approach has proven its value in our study in formulating GY-prediction models. However, an implicit limitation of shovelomics is that, besides crown root informing traits, this methodological approach does not allow a clear inference of the root architecture throughout the soil profile. This is why soil core-derived traits have been used as an extension to root studies at given soil depths, with root length density (total root length per unit soil volume) as the main determined trait (Chen et al., 2017; Elazab et al., 2012; Foulkes et al., 2009; York et al., 2018b). A higher root length density at soil depth has been reported to improve the capture of belowground resources under drought stress in wheat (Foulkes et al., 2009; Manschadi et al., 2006; Reynolds et al., 2007). However, a larger root system is not necessarily related to higher aerial biomass and yield. Thus, our study showed that core traits such as RDW, $Area_{roots}$ and Area/RDW, for the different soil sections were negatively correlated with GY across seasons, under INP, as well as all the agronomic conditions combined. In this sense, Elazab et al. (2016) working with durum wheat in lysimeters concluded that under water stress, aerial biomass was negatively correlated with root dry biomass, root length and root length density and positively correlated with the specific root length.

Except for the severe dry season (2018–2019), our results suggest that regardless of the observed effects of growing conditions (water regimen and planting date) and seasons affect total RDW across soil sections, and that root biomass decreases at depth, the $Area_{roots}$, as an indicator of root functionality, remained rather constant across the one metre depth soil profile studied. This was achieved by roots becoming progressively thinner (lower Area/RDW) as they moved down through the soil profile. In fact, thinner roots or roots with higher specific root length have been reported as possessing positive traits in terms of wheat performance, not only under lysimeter setups (Elazab et al., 2012, 2016) but also under field conditions (Barraclough et al., 1989; Corneo et al., 2016; Peng et al., 2019; Rezzouk et al., 2022). In addition, the constancy in $Area_{roots}$ across soil sections supports the possible existence of a dual root system for all the growing conditions, with the presence of a shallow and deep rooting system (Bai et al., 2019; Rezzouk et al., 2022). However, soil coring, particularly under field conditions, is by no means a high throughput methodology, and is prone to errors associated with separating the fine roots from the soil. Moreover, root architecture does not necessarily directly inform about root functioning. This is why our study also evaluated the $\delta^{18}O$ and $\delta^{2}H$ of the stem base water as a phenotyping alternative to assess root functioning.

The negative correlation of $\delta^{18}O_{stem}$ and $\delta^{2}H_{stem}$ with GY of both rainfed and support irrigation normal planting trials suggests that genotypes that are capable of exploring water and related resources (e.g. nitrogen) deeper in soil profiles are the most productive. This was further supported by the correlations of $\delta^{18}O_{stem}$ with CTD (negative), $\delta^{13}C$ (positive) and $\delta^{15}N$ (negative), particularly under RNP conditions. In fact, the isotope signatures of $\delta^{18}O$ and $\delta^{2}H$ in stem water have been used for decades in plant ecology and physiology as an approach to studying soil-plant water movements in woody and herbaceous plants (Barbour, 2007; Zhang et al., 2017; Hirl et al., 2019). The rationality of the approach is simple overall, with the $\delta^{18}O$ and $\delta^{2}H$ of the soil water increasing in response to the effect of evaporation, while the deeper the water's location in the soil the less exposed it is to evaporation (Barbour, 2007; DeNiro and Epstein, 1979; Mateo et al., 2004). On the other hand, the approach assumes that no evaporation (thus isotopic fractionation) occurs once the water is captured and further transported by the root xylem (Cernusak et al., 2016; Dawson and Ehleringer, 1993). However, in recent years these methods have been challenged, claiming that factors such as the cryogenic method applied in the stem water extraction (Chen et al., 2020) and the temperature of water extraction (Millar et al., 2018) cause source-stem isotopic offsets, while the soil's moisture conditions may also cause offsets, particularly as the soil became drier (Barbeta et al., 2020). However, these offsets were more evident for $\delta^{2}H$, while in the case of $\delta^{18}O$, various studies have reported differences between the isotopic signal of the stem ($\delta^{18}O_{stem}$) and the water source ($\delta^{18}O_{source}$) ranging from insignificant to almost nothing (Barbeta et al., 2020; Chen et al., 2020; de Deurwaerder et al., 2020).

Besides the extraction methods, recent studies have reported that growing conditions are also factors to consider when assessing water stable isotopes. In fact, in herbaceous plants, $\delta^{2}H_{xylem}$ and $\delta^{18}O_{xylem}$ were affected by CVD conditions when grown in clayey soils whereas in sandy soils the isotopes were unaffected (Orlowski et al., 2018). In the current work, the experimentation site was predominantly sandy (Supplemental Table 2). In accordance with the reliability of the method, $\delta^{18}O_{stem}$ not only correlated consistently with CTD, $\delta^{13}C$ and GY (Fig. 4) but also was within the range of $\delta^{18}O_{source}$ values of the soil profile (Fig. 3) and was consistently placed opposite GY within the PCAs for each of the two seasons where $\delta^{18}O_{stem}$ was analysed (Supplemental Fig. 1). These results agree with and further support the reliability of $\delta^{18}O$ for tracking the water source (Barbeta et al., 2020, 2022; Chen et al., 2020; Rezzouk et al., 2022; Rothfuss and Javaux, 2017). On the

other hand, δ^2H_{stem} exhibited a more erratic pattern alongside weaker correlations with GY and related traits (Supplemental Table 10).

Under INP, the negative relationship of the Area/RDW ratio at 50–70 cm with the $\delta^{18}O$ and δ^2H of the stem water supports the idea that thinner roots in deeper soil sections are the most functional at extracting water. In the same way, the shovelomic trait informing about root thickness (Rwidth) was also negatively correlated with $\delta^{18}O$ and δ^2H. In addition, RA was also positively correlated with $\delta^{18}O$ and δ^2H, which supports the concept that the steeper the roots, the greater the depth of water extraction. Under RNP conditions, $Area_{roots\ 50–75\ cm}$ was negatively correlated with $\delta^{18}O_{stem}$, suggesting that roots captured water from deeper soil sections. In addition, the shovelomic indicator of tendency to higher root density at depth (Ldist) was negatively correlated with the isotope composition of stem water, which also suggests deeper water extraction under rainfed conditions. In fact, within rainfed conditions, the isotope composition of the soil water clearly decreased with soil depth. The pattern of $\delta^{18}O_{soil}$ and δ^2H_{soil} throughout the soil profile further supports the dual pattern of the root system under support irrigation conditions, while under rainfed conditions, root architecture optimises water extraction at depth.

5. Conclusion

The four crop management settings combined with the four consecutive seasons included in this study covered a wide range of grain yield scenarios within the Mediterranean region. However, in all cases higher GY was associated with stronger growth (higher PH) and larger green biomass that was maintained longer during grain filling (higher NDVI). Moreover, in almost all cases, greater crop growth was positively associated with a more effective use of resources, particularly water, as inferred from the higher transpiration (higher CTD) and stomatal conductance (lower $\delta^{13}C$), and to a lesser extent nitrogen, as concluded from the higher nitrogen accumulation (higher GNY and N_{leaf} concentration) associated with a greater demand for nitrogen from the soil (higher $\delta^{15}N$). This study highlights the highly plastic nature of wheat root architecture when adapting to different Mediterranean conditions, with RNP conditions inducing deeper root systems, INP presenting a more dual root system (superficial as well as deeper), while ILP and even RLN exhibited more superficial root systems. Nevertheless, our study also highlights the limitation of shovelomics. Thus, soil coring suggests that a constancy in root area is achieved by crops throughout the agricultural soil profile, except for severe drought conditions. However, the information derived on root architecture is not necessarily linked to root functioning. On the other hand, the $\delta^{18}O$ and δ^2H of the stem water appear as a potential phenotyping functional approach to select crops that are better adapted to Mediterranean conditions, despite some concerns about their applicability, particularly regarding δ^2H. In our study, the negative relationship of $\delta^{18}O$ and δ^2H to GY suggests that the most productive crops take water up from deeper soil sections, which makes this approach relatively high throughput for selecting for more efficient root systems. This is particularly evident for the rainfed trials, where a clear gradient from a less to a more negative stable isotope composition of soil water was established across soil depths. In the case of support irrigation trials, the gradient was less obvious, which implies that extracting water from deeper soil sections is not necessarily the issue.

CRediT authorship contribution statement

FZR wrote the first draft, collected samples, assessed the shovelomics and soil coring root traits, analysed thermal and root images, conducted stable isotope and statistical analyses, drew the tables and figures, and implemented edits under the supervision of JLA and MDS; JLA, MDS and NA conceived and designed the experiment. JLA and MDS revised the draft and implemented edits in the consecutive drafts; NA conducted the field trials and coordinated the agronomic and soil coring data collection. AGR and SCK conducted the flights for thermal imaging. SCK developed the FIJI codes for the analysis of thermal and scanned root images. FZR, JS, JLA and NA collaborated to isolate root cores. All authors collaborated in field data assessment.

Declaration of Competing Interest

The authors declare that they have no known competing financial interests or personal relationships that could have appeared to influence the work reported in this paper..

Data Availability

Data will be made available on request.

Acknowledgments

This study was supported by the Spanish Project PID2019-106650RB-C2 from the Ministerio de Ciencia e Innovación. JLA acknowledges support from the Catalan Institution for Research and Advanced Studies, Generalitat de Catalunya, Spain, through its ICREA Academia program. FZR was a recipient of a research grant (FI-AGAUR) sponsored by the Agency for Management of University and Research Grants (AGAUR), in collaboration with the University of Barcelona. SCK was supported by the Ramon y Cajal RYC-2019-027818-I research fellowship from the Ministerio de Ciencia e Innovación, Spain. AGR was funded by a Margarita Salas post-doctoral contract from the Spanish Ministry of Universities affiliated with the Research Vice-Rector of the University of Barcelona. We thank members of the Integrative Crop Ecophysiology Group of the University of Barcelona and the personnel from the experimental station of ITACYL at Zamadueñas (Valladolid) for their assistance during the study's data assessments. We extend our thanks to The Water Research Institute (IdRA) for their financial support to cover laboratory analyses. We thank Dr. J. Voltas from the University of Lleida, Spain, for his support with the $\delta^{18}O$ and δ^2H water analyses.

Appendix A. Supporting information

Supplementary data associated with this article can be found in the online version at doi:10.1016/j.agwat.2023.108487.

References

Akram, Z., Ajmal, S.U., Munir, M., 2008. Estimation of correlation coefficient among some yield parameters of wheat under rainfed conditions. Pak. J. Bot. 40, 1777–1781.

Aparicio, N., Villegas, D., Casadesus, J., Araus, J.L., Royo, C., 2000. Spectral vegetation indices as nondestructive tools for determining durum wheat yield. Agron. J. 92, 83–91. https://doi.org/10.2134/agronj2000.92183x.

Araus, J.L., Cabrera-Bosquet, L., Serret, M.D., Bort, J., Nieto-Taladriz, M.T., 2013. Comparative performance of $\delta^{13}C$, $\delta^{18}O$ and $\delta^{15}N$ for phenotyping durum wheat adaptation to a dryland environment. Funct. Plant Biol. 40, 595–608. https://doi.org/10.1071/FP12254.

Araus, J.L., Cairns, J.E., 2014. Field high-throughput phenotyping: the new crop breeding frontier. Trends Plant Sci. 19, 52–61. https://doi.org/10.1016/j.tplants.2013.09.008.

Araus, J.L., Slafer, G.A., 2011. Crop stress management and global climate change. In: Crop Stress Management and Global Climate Change, Vol 2. CABI, pp. 1–210. https://doi.org/10.1079/9781845936808.0000.

Araus, J.L., Villegas, D., Aparicio, N., Garcıa del Moral, L.F., El-Hani, S., Rharrabti, Y., Ferrio, J.P., Royo, C., 2003. Environmental factors determining carbon isotope discrimination and yield in durum wheat under Mediterranean conditions. Crop Sci. 43, 170–180. https://doi.org/10.2135/cropsci2003.0170.

Araus, J.L., Slafer, G.A., Royo, C., Serret, M.D., 2008. Breeding for yield potential and stress adaptation in cereals. Crit. Rev. Plant Sci 377–412. https://doi.org/10.1080/07352680802467736.

Araus, Jose Luis, Kefauver, S.C., Vergara-Díaz, O., Gracia-Romero, A., Rezzouk, F.Z., Segarra, J., Buchaillot, M.L., Chang-Espino, M., Vatter, T., Sanchez-Bragado, R., Fernandez-Gallego, J.A., Serret, M.D., Bort, J., 2022. Crop phenotyping in a context of global change: what to measure and how to do it. J. Integr. Plant Biol. 64, 592–618. https://doi.org/10.1111/jipb.13191.

Armengaud, P., 2009. EZ-Rhizo software: The gateway to root architecture analysis. Plant Signal. Behav. 4, 139–141. https://doi.org/10.4161/psb.4.2.7763.

Asins, M.J., Carbonell, E.A., 1989. Distribution of genetic variability in a durum wheat world collection. Theor. Appl. Genet. 77, 287–294. https://doi.org/10.1007/BF00266199.

Bai, C., Ge, Y., Ashton, R.W., Evans, J., Milne, A., Hawkesford, M.J., Whalley, W.R., Parry, M.A.J., Melichar, J., Feuerhelm, D., Basler, P.B., Bartsch, M., 2019. The relationships between seedling root screens, root growth in the field and grain yield for wheat. Plant Soil 440, 311–326. https://doi.org/10.1007/s11104-019-04088-9.

Barbeta, A., Gimeno, T.E., Clavé, L., Fréjaville, B., Jones, S.P., Delvigne, C., Wingate, L., Ogée, J., 2020. An explanation for the isotopic offset between soil and stem water in a temperate tree species. New Phytol. 227, 766–779. https://doi.org/10.1111/nph.16564.

Barbeta, A., Burlett, R., Martín-Gómez, P., Fréjaville, B., Devert, N., Wingate, L., Domec, J.C., Ogée, J., 2022. Evidence for distinct isotopic compositions of sap and tissue water in tree stems: consequences for plant water source identification. New Phytol. 233, 1121–1132. https://doi.org/10.1111/nph.17857.

Barbour, M.M., 2007. Stable oxygen isotope composition of plant tissue: a review. Funct. Plant Biol. 34, 83–94. https://doi.org/10.1071/FP06228.

Barraclough, P.B., Weir, A.H., 1988. Effects of a compacted subsoil layer on root and shoot growth, water use and nutrient uptake of winter wheat. J. Agric. Sci. 110, 207–216. https://doi.org/10.1017/S0021859600081235.

Barraclough, P.B., Kuhlmann, H., Weir, A.H., 1989. The effects of prolonged drought and nitrogen fertilizer on root and shoot growth and water uptake by winter wheat. J. Agron. Crop Sci. 163, 352–360. https://doi.org/10.1111/j.1439-037X.1989.tb00778.x.

Bendig, J., Bolten, A., Bennertz, S., Broscheit, J., Eichfuss, S., Bareth, G., 2014. Estimating biomass of barley using crop surface models (CSMs) derived from UAV-based RGB imaging. Remote Sens. 6, 10395–10412. https://doi.org/10.3390/rs61110395.

Berry, Z.C., Emery, N.C., Gotsch, S.G., Goldsmith, G.R., 2019. Foliar water uptake: processes, pathways, and integration into plant water budgets. Plant Cell Environ. 42, 410–423. https://doi.org/10.1111/pce.13439.

Blum, A., 2009. Effective use of water (EUW) and not water-use efficiency (WUE) is the target of crop yield improvement under drought stress. Field Crop. Res. 112, 119–123. https://doi.org/10.1016/j.fcr.2009.03.009.

Blum, A., Sullivan, C.Y., 1997. The effect of plant size on wheat response to agents of drought stress. I. root drying. J. Plant Physiol. 24, 35–41. https://doi.org/10.1071/PP96022.

Boudiar, R., Cabeza, A., Fernández-Calleja, M., Pérez-Torres, A., Casas, A.M., González, J.M., Mekhlouf, A., Igartua, E., 2021. Root trait diversity in field grown durum wheat and comparison with seedlings. Agronomy 11, 1–18. https://doi.org/10.3390/agronomy11122545.

Box Jnr, J.E., Ramseur, E.L., 1993. Minirhizotron wheat root data: Comparisons to soil core root data. Agron. J. 85, 1058–1060. https://doi.org/10.2134/agronj1993.00021962008500050019x.

Bucksch, A., Burridge, J., York, L.M., Das, A., Nord, E., Weitz, J.S., Lynch, J.P., 2014. Image-based high-throughput field phenotyping of crop roots. Plant Physiol. 166, 470–486. https://doi.org/10.1104/pp.114.243519.

Cabrera-Bosquet, L., Molero, G., Stellacci, A., Bort, J., Nogués, S., Araus, J., 2011. NDVI as a potential tool for predicting biomass, plant nitrogen content and growth in wheat genotypes subjected to different water and nitrogen conditions. Cereal Res. Commun. 39, 147–159. https://doi.org/10.1556/crc.39.2011.1.15.

Ceglar, A., Toreti, A., Zampieri, M., Royo, C., 2021. Global loss of climatically suitable areas for durum wheat growth in the future. Environ. Res. Lett. 16, 1–12. https://doi.org/10.1088/1748-9326/ac2d68.

Centro de Estudios y Experimentación de Obras Públicas (CEDEX), 2022. ⟨https://www.cedex.es/centros-laboratorios/centro-estudios-tecnicas-aplicadas-ceta/lineas-actividad/diseno-metodologia-muestreo-analisis⟩ (Accessed April 11th, 2023).

Cernusak, L.A., Barbour, M.M., Arndt, S.K., Cheesman, A.W., English, N.B., Feild, T.S., Helliker, B.R., Holloway-Phillips, M.M., Holtum, J.A.M., Kahmen, A., Mcinerney, F. A., Munksgaard, N.C., Simonin, K.A., Song, X., Stuart-Williams, H., West, J.B., Farquhar, G.D., 2016. Stable isotopes in leaf water of terrestrial plants. Plant Cell Environ. 39, 1087–1102. https://doi.org/10.1111/pce.12703.

Chairi, F., Vergara-Diaz, O., Vatter, T., Aparicio, N., Nieto-Taladriz, M.T., Kefauver, S.C., Bort, J., Serret, M.D., Araus, J.L., 2018. Post-green revolution genetic advance in durum wheat: the case of Spain. Field Crop. Res. 228, 158–169. https://doi.org/10.1016/j.fcr.2018.09.003.

Chairi, F., Aparicio, N., Serret, M.D., Araus, J.L., 2020. Breeding effects on the genotype × environment interaction for yield of durum wheat grown after the green revolution: the case of Spain. Crop J. 8, 623–634. https://doi.org/10.1016/j.cj.2020.01.005.

Chapman, S.C., Chakraborty, S., Dreccer, M.F., Howden, S.M., 2012. Plant adaptation to climate change-opportunities and priorities in breeding. Crop Pasture. Sci 63, 251–268. https://doi.org/10.1071/CP11303.

Chen, X., Ding, Q., Błaszkiewicz, Z., Sun, J., Sun, Q., He, R., Li, Y., 2017. Phenotyping for the dynamics of field wheat root system architecture. Sci. Rep. 7, 1–11. https://doi.org/10.1038/srep37649.

Chen, Y., Helliker, B.R., Tang, X., Li, F., Zhou, Y., Song, X., 2020. Stem water cryogenic extraction biases estimation in deuterium isotope composition of plant source water. Proc. Natl. Acad. Sci. USA 117, 33345–33350. https://doi.org/10.1073/PNAS.2014422117.

Chochois, V., Voge, J.P., Rebetzke, G.J., Watt, M., 2015. Variation in adult plant phenotypes and partitioning among seed and stem-borne roots across Brachypodium distachyon accessions to exploit in breeding cereals for well-watered and drought environments. Plant Physiol. 168, 953–967. https://doi.org/10.1104/pp.15.00095.

Choi, W., Ro, H., Lee, S., 2003. Natural 15 N abundances of inorganic nitrogen in soil treated with fertilizer and compost under changing soil moisture regimes. Soil Biol. Chem. 35, 1289–1298. https://doi.org/10.1016/S0038-0717(03)00199-8.

Christopher, J.T., Manschadi, A.M., Hammer, G.L., Borrell, A.K., 2008. Developmental and physiological traits associated with high yield and stay-green phenotype in wheat. Aust. J. Agric. Res. 59, 354–364. https://doi.org/10.1071/AR07193.

Christopher, J.T., Veyradier, M., Borrell, A.K., Harvey, G., Fletcher, S., Chenu, K., 2014. Phenotyping novel stay-green traits to capture genetic variation in senescence dynamics. Funct. Plant Biol. 41, 1035–1048. https://doi.org/10.1071/FP14052.

Christopher, J.T., Christopher, M.J., Borrell, A.K., Fletcher, S., Chenu, K., 2016. Stay-green traits to improve wheat adaptation in well-watered and water-limited environments. J. Exp. Bot. 67, 5159–5172. https://doi.org/10.1093/jxb/erw276.

Clark, R.T., MacCurdy, R.B., Jung, J.K., Shaff, J.E., McCouch, S.R., Aneshansley, D.J., Kochian, L.V., 2011. Three-dimensional root phenotyping with a novel imaging and software platform. Plant Physiol. 156, 455–465. https://doi.org/10.1104/pp.110.169102.

Condon, A.G., 2020. Drying times: plant traits to improve crop water use efficiency and yield. J. Exp. Bot. 71, 2239–2252. https://doi.org/10.1093/jxb/eraa002.

Corneo, P.E., Suenaga, H., Kertesz, M.A., Dijkstra, F.A., 2016. Effect of twenty four wheat genotypes on soil biochemical and microbial properties. Plant Soil 404, 141–155. https://doi.org/10.1007/s11104-016-2833-1.

Cossani, C.M., Slafer, G.A., Savin, R., 2010. Co-limitation of nitrogen and water, and yield and resource-use efficiencies of wheat and barley. Crop Pasture Sci. 61, 844–851. https://doi.org/10.1071/CP10018.

Dainelli, R., Calmanti, S., Pasqui, M., Rocchi, L., Di Giuseppe, E., Monotti, C., Quaresima, S., Matese, A., Di Gennaro, S.F., Toscano, P., 2022. Moving climate seasonal forecasts information from useful to usable for early within-season predictions of durum wheat yield. Clim. Serv. 28, 100324 https://doi.org/10.1016/j.cliser.2022.100324.

Dawson, T.E., Ehleringer, J.R., 1993. Isotopic enrichment of water in the "woody" tissues of plants: Implications for plant water source, water uptake, and other studies which use the stable isotopic composition of cellulose. Geochim. Cosmochim. Acta 57, 3487–3492. https://doi.org/10.1016/0016-7037(93)90554-A.

Dawson, T.E., Goldsmith, G.R., 2018. The value of wet leaves. New Phytol. 219, 1156–1169. https://doi.org/10.1111/nph.15307.

DeNiro, M.J., Epstein, S., 1979. Relationship between the oxygen Isotope ratios of terrestrial. Science 204, 51–53. https://doi.org/10.1126/science.204.4388.51.

de Deurwaerder, H., Visser, M., Detto, M., Boeckx, P., Meunier, F., Zhao, L., Wang, L., Verbeeck, H., 2020. Diurnal variation in the isotope composition of plant xylem water biases the depth of root-water uptake estimates. Biogeosci. Discuss Preprint 1–48.

Elazab, A., Molero, G., Serret, M.D., Araus, J.L., 2012. Root traits and $\delta^{13}C$ and $\delta^{18}O$ of durum wheat under different water regimes. Funct. Plant Biol. 39, 379–393. https://doi.org/10.1071/FP11237.

Elazab, A., Serret, M.D., Araus, J.L., 2016. Interactive effect of water and nitrogen regimes on plant growth, root traits and water status of old and modern durum wheat genotypes. Planta 244, 125–144. https://doi.org/10.1007/s00425-016-2500-z.

Fageria, N.K., Moreira, A., 2011. The role of mineral nutrition on root growth of crop plants. Advances in Agronomy, first ed. Elsevier Inc. https://doi.org/10.1016/B978-0-12-385531-2.00004-9.

Farquhar, G.D., Ehleringer, J.R., Hubick, K.T., 1989. Carbon isotope discrimination and photosynthesis. Annu. Rev. Plant Physiol. 40, 503–537. https://doi.org/10.1146/annurev.pp.40.060189.002443.

Farquhar, G.D., Richards, R.A., 1984. Isotopic composition of plant carbon correlates with water-use efficiency of wheat genotypes. Australian Journal of Plant Physiology 11, 539–552. https://doi.org/10.1071/PP9840539.

Ferrise, R., Moriondo, M., Bindi, M., 2011. Probabilistic assessments of climate change impacts on durum wheat in the Mediterranean region. Nat. Hazard. Earth Syst. Sci. 11, 1293–1302. https://doi.org/10.5194/nhess-11-1293-2011.

Fischer, R.A., 2011. Wheat physiology: a review of recent developments. Crop Pasture Sci. 62, 95–114. https://doi.org/10.1071/CP10344.

Fischer, R.A., Rees, D., Sayre, K.D., Lu, Z.M., Condon, A.G., Larque Saavedra, A., 1998. Wheat yield progress associated with higher stomatal conductance and photosynthetic rate, and cooler canopies. Crop Sci. 38, 1467–1475. https://doi.org/10.2135/cropsci1998.0011183×003800060011x.

Foulkes, M.J., Hawkesford, M.J., Barraclough, P.B., Holdsworth, M.J., Kerr, S., Kightley, S., Shewry, P.R., 2009. Identifying traits to improve the nitrogen economy of wheat: recent advances and future prospects. Field Crop. Res. 114, 329–342. https://doi.org/10.1016/j.fcr.2009.09.005.

Fradgley, N., Evans, G., Biernaskie, J.M., Cockram, J., Marr, E.C., Oliver, A.G., Ober, E., Jones, H., 2020. Effects of breeding history and crop management on the root architecture of wheat. Plant Soil 452, 587–600. https://doi.org/10.1007/s11104-020-04585-2.

Galkovskyi, T., Mileyko, Y., Bucksch, A., Moore, B., Symonova, O., Price, C.A., Topp, C. N., Iyer-Pascuzzi, A.S., Zurek, P., Fang, S., Harer, J., Benfey, P.N., Weitz, J.S., 2012. GiA Roots: software for the high throughput analysis of plant root system architecture. BMC Plant Biol. 12, 1–54. https://doi.org/10.1186/1471-2229-12-116.

Guzmán, C., Autrique, J.E., Mondal, S., Singh, R.P., Govindan, V., Morales-Dorantes, A., Posadas-Romano, G., Crossa, J., Ammar, K., Peña, R.J., 2016. Response to drought and heat stress on wheat quality, with special emphasis on bread-making quality, in durum wheat. Field Crop. Res. 186, 157–165. https://doi.org/10.1016/j.fcr.2015.12.002.

Haberle, J., Svoboda, P., Raimanová, I., 2008. The effect of post-anthesis water supply on grain nitrogen concentration and grain nitrogen yield of winter wheat. Plant Soil Environ. 54, 304–312. https://doi.org/10.17221/422-pse.

He, M., Jiang, Y., Liu, L., Zhong, X., Zhao, Y., Ma, W., Tang, G., 2022. Benefits of high nitrogen fertilizer on nitrogen metabolism, nitrogen transfer rate, root system architecture and grain yield of wheat (Triticum aestivum L.) under water deficit at heading stage. Act. Physiol. Plant 44, 1–10. https://doi.org/10.1007/s11738-022-03460-0.

Hernandez-Ochoa, I.M., Luz Pequeno, D.N., Reynolds, M., Babar, M.A., Sonder, K., Milan, A.M., Hoogenboom, G., Robertson, R., Gerber, S., Rowland, D.L., Fraisse, C. W., Asseng, S., 2019. Adapting irrigated and rainfed wheat to climate change in semi-arid environments: management, breeding options and land use change. Eur. J. Agron. 109, 1–11. https://doi.org/10.1016/j.eja.2019.125915.

Hirl, R.T., Schnyder, H., Ostler, U., Schäufele, R., Schleip, I., Vetter, S.H., Auerswald, K., Baca Cabrera, J.C., Wingate, L., Barbour, M.M., Ogée, J., 2019. The 18O ecohydrology of a grassland ecosystem–predictions and observations. Hydrol. Earth Syst. Sci. 23 (6), 2581–2600.

Hodge, A., 2009. Root decisions. Plant Cell Environ. 32, 628–640. https://doi.org/10.1111/j.1365-3040.2008.01891.x.

Hodgkinson, L., Dodd, I.C., Binley, A., Ashton, R.W., White, R.P., Watts, C.W., Whalley, W.R., 2017. Root growth in field-grown winter wheat: Some effects of soil conditions, season and genotype. Eur. J. Agron. 91, 74–83. https://doi.org/10.1016/j.eja.2017.09.014.

Hoffmann, M.P., Haakana, M., Asseng, S., Höhn, J.G., Palosuo, T., Ruiz-Ramos, M., Fronzek, S., Ewert, F., Gaiser, T., Kassie, B.T., Paff, K., Rezaei, E.E., Rodríguez, A., Semenov, M., Srivastava, A.K., Stratonovitch, P., Tao, F., Chen, Y., Rötter, R.P., 2018. How does inter-annual variability of attainable yield affect the magnitude of yield gaps for wheat and maize? An analysis at ten sites. Agric. Syst. 159, 199–208. https://doi.org/10.1016/j.agsy.2017.03.012.

Iyer-Pascuzzi, A.S., Symonova, O., Mileyko, Y., Hao, Y., Belcher, H., Harer, J., Weitz, J.S., Benfey, P.N., 2010. Imaging and analysis platform for automatic phenotyping and trait ranking of plant root systems. Plant Physiol. 152, 1148–1157. https://doi.org/10.1104/pp.109.150748.

Joshi, A.K., Kumari, M., Singh, V.P., Reddy, C.M., Kumar, S., Rane, J., Chand, R., 2007.). Stay green trait: variation, inheritance and its association with spot blotch resistance in spring wheat (Triticum aestivum L.). Euphytica 153, 59–71. https://doi.org/10.1007/s10681-006-9235-z.

Kale Çelik, S., Madenoğlu, S., Sönmez, B., Avağ, K., Türker, U., Çayci, G., Kütük, A.C., Heng, L.K., 2018. Oxygen isotope discrimination of wheat and its relationship with yield and stomatal conductance under irrigated conditions. Turk. J. Agric. 42, 22–28. https://doi.org/10.3906/tar-1709-31.

Kätterer, T., Hansson, A.C., Andrén, O., 1993. Wheat root biomass and nitrogen dynamics-effects of daily irrigation and fertilization. Plant Soil 151, 21–30. https://doi.org/10.1007/BF00010782.

Kefauver, S.C., Vicente, R., Vergara-Díaz, O., Fernandez-Gallego, J.A., Kerfal, S., Lopez, A., Melichar, J.P.E., Serret Molins, M.D., Araus, J.L., 2017. Comparative UAV and field phenotyping to assess yield and nitrogen use efficiency in hybrid and conventional barley. Front. Plant Sci. https://doi.org/10.3389/fpls.2017.01733.

Khaliq, I., Parveen, N., Chowdhry, M.A., 2004. Correlation and path coefficient analyses in bread wheat. Int. J. Agric. Biol. 6, 633–635.

Kipp, S., Mistele, B., Schmidhalter, U., 2014. Identification of stay-green and early senescence phenotypes in high-yielding winter wheat, and their relationship to grain yield and grain protein concentration using high-throughput phenotyping techniques. Funct. Plant Biol. 41, 227–235. https://doi.org/10.1071/FP13221.

Kirkegaard, J.A., Lilley, J.M., 2007. Root penetration rate - a benchmark to identify soil and plant limitations to rooting depth in wheat. Aust. J. Exp. Agric. 47, 590–602. https://doi.org/10.1071/EA06071.

Kong, X., Zhang, M., De Smet, I., Ding, Z., 2014. Designer crops: optimal root system architecture for nutrient acquisition. Trends Biotechnol. 32, 597–598. https://doi.org/10.1016/j.tibtech.2014.09.008.

Li, X., Ingvordsen, C.H., Weiss, M., Rebetzke, G.J., Condon, A.G., James, R.A., Richards, R.A., 2019. Deeper roots associated with cooler canopies, higher normalized difference vegetation index, and greater yield in three wheat populations grown on stored soil water. J. Exp. Bot. 70, 4963–4974. https://doi.org/10.1093/jxb/erz232.

Lopes, M.S., Reynolds, M.P., 2010. Partitioning of assimilates to deeper roots is associated with cooler canopies and increased yield under drought in wheat. Funct. Plant Biol. 37, 147–156. https://doi.org/10.1071/FP09121.

Lopes, M.S., Reynolds, M.P., 2012. In Posidonia oceanica cadmium induces changes in DNA Stay-green in spring wheat can be determined by spectral reflectance measurements (normalized difference vegetation methylation and chromatin patterning index) independently from phenology. J. Exp. Bot. 63, 695–709. https://doi.org/10.1093/jxb/err313.

Lynch, J., 1995. Root architecture and plant productivity. Plant Physiol. 109, 7–13. https://doi.org/10.1104/pp.109.1.7.

Lynch, J.P., 2013. Steep, cheap and deep: an ideotype to optimize water and N acquisition by maize root systems. Ann. Bot. 112, 347–357. https://doi.org/10.1093/aob/mcs293.

Maccaferri, M., El-Feki, W., Nazemi, G., Salvi, S., Canè, M.A., Colalongo, M.C., Stefanelli, S., Tuberosa, R., 2016. Prioritizing quantitative trait loci for root system architecture in tetraploid wheat. J. Exp. Bot. 67, 1161–1178. https://doi.org/10.1093/jxb/erw039.

Malamy, J.E., 2005. Intrinsic and environmental response pathways that regulate root system architecture. Plant Cell Environ. 1, 67–77. https://doi.org/10.1111/j.1365-3040.2005.01306.x.

Manschadi, A.M., Christopher, J., Devoil, P., Hammer, G.L., 2006. The role of root architectural traits in adaptation of wheat to water-limited environments. Funct. Plant Biol. 33, 823–837. https://doi.org/10.1071/FP06055.

Manschadi, A.M., Christopher, J.T., Hammer, G.L., Devoil, P., 2010.). Experimental and modelling studies of drought-adaptive root architectural traits in wheat (Triticum aestivum L.). Plant Biosyst. 144, 458–462. https://doi.org/10.1080/11263501003731805.

Marti, J., Bort, J., Slafer, G.A., Araus, J.L., 2007. Can wheat yield be assessed by early measurements of normalized difference vegetation index. Ann. Appl. Biol. 150, 253–257. https://doi.org/10.1111/j.1744-7348.2007.00126.x.

Martínez-Moreno, F., Solís, I., Noguero, D., Blanco, A., Özberk, İ., Nsarellah, N., Elias, E., Mylonas, I., Soriano, J.M., 2020. Durum wheat in the Mediterranean Rim: historical evolution and genetic resources. Genet. Resour. Crop Evol. 67, 1415–1436. https://doi.org/10.1007/s10722-020-00913-8.

Martín-Gómez, P., Barbeta, A., Voltas, J., Peñuelas, J., Dennis, K., Palacio, S., Dawson, T. E., Ferrio, J.P., 2015. Isotope-ratio infrared spectroscopy: a reliable tool for the investigation of plant-water sources? N. Phytol. 207, 914–927. https://doi.org/10.1111/nph.13376.

Mateo, M.A., Ferrio, P., Araus, J.L., 2004. Isótopos estables en fisiología vegetal. In: Reigosa, M.J., Pedrol, N., Sánchez, A. (Eds.), La ecofisiología vegetal, una ciencia de síntesis. Paranimfo, S.A, pp. 1–38.

Millar, C., Pratt, D., Schneider, D.J., McDonnell, J.J., 2018. A comparison of extraction systems for plant water stable isotope analysis. Rapid Commun. Mass Spectrom. 32, 1031–1044. https://doi.org/10.1002/rcm.8136.

Narayanan, S., Mohan, A., Gill, K.S., Vara Prasad, P.V., 2014. Variability of root traits in spring wheat germplasm. PLoS One 9, 1–15. https://doi.org/10.1371/journal.pone.0100317.

Nehe, A.S., Foulkes, M.J., Ozturk, I., Rasheed, A., York, L., Kefauver, S.C., Ozdemir, F., Morgounov, A., 2021. Root and canopy traits and adaptability genes explain drought tolerance responses in winter wheat. PLoS One 16, 1–25. https://doi.org/10.1371/journal.pone.0242472.

Ober, E.S., Alahmad, S., Cockram, J., Forestan, C., Hickey, L.T., Kant, J., Maccaferri, M., Marr, E., Milner, M., Pinto, F., Rambla, C., Reynolds, M., Salvi, S., Sciara, G., Snowdon, R.J., Thomelin, P., Tuberosa, R., Uauy, C., Voss-Fels, K.P., Wallington, E., Watt, M., 2021. Wheat root systems as a breeding target for climate resilience. Theor. Appl. Genet. 134, 1645–1662. https://doi.org/10.1007/s00122-021-03819-w.

Orlowski, N., Winkler, A., McDonnell, J.J., Breuer, L., 2018. A simple greenhouse experiment to explore the effect of cryogenic water extraction for tracing plant source water. Ecohydrology 11, 1–12. https://doi.org/10.1002/eco.1967.

Padovan, G., Martre, P., Semenov, M.A., Masoni, A., Bregaglio, S., Ventrella, D., Lorite, I. J., Santos, C., Bindi, M., Ferrise, R., Dibari, C., 2020. Understanding effects of genotype × environment × sowing window interactions for durum wheat in the Mediterranean basin. Field Crop. Res. 259, 1–15. https://doi.org/10.1016/j.fcr.2020.107969.

Paez-Garcia, A., Motes, C.M., Scheible, W.R., Chen, R., Blancaflor, E.B., Monteros, M.J., 2015. Root traits and phenotyping strategies for plant improvement. Plants 4, 334–355. https://doi.org/10.3390/plants4020334.

Pask, A.J.D., Pietragalla, J., Mullan, D.M. Reynolds, M.P. (Eds.) (2012) Physiological breeding II: A field guide to wheat phenotyping. Mexico, D.F.: CIMMYT. http://onlinelibrary.wiley.com/doi/10.1002/cbdv.200490137/abstract%0Ahttps://www.cambridge.org/core/product/identifier/CBO9781107415324A009/type/book_part.

Passioura, J.B., 1983. Roots and drought resistance. Agric. Water Manag. 12, 265–280. https://doi.org/10.1016/b978-0-444-42214-9.50025-9.

Peng, B., Liu, X., Dong, X., Xue, Q., Neely, C.B., Marek, T., Ibrahim, A.M.H., Zhang, G., Leskovar, D.I., Rudd, J.C., 2019. Root morphological traits of winter wheat under contrasting environments. J. Agron. Crop Sci. 205, 571–585. https://doi.org/10.1111/jac.12360.

Pinto, R.S., Reynolds, M.P., 2015. Common genetic basis for canopy temperature depression under heat and drought stress associated with optimized root distribution in bread wheat. Theor. Appl. Genet. 128, 575–585. https://doi.org/10.1007/s00122-015-2453-9.

Reynolds, M., Dreccer, F., Trethowan, R., 2007. Drought-adaptive traits derived from wheat wild relatives and landraces. J. Exp. Bot. 58, 177–186. https://doi.org/10.1093/jxb/erl250.

Rezzouk, F.Z., Gracia-Romero, A., Kefauver, S.C., Gutiérrez, N.A., Aranjuelo, I., Serret, M.D., Araus, J.L., 2020. Remote sensing techniques and stable isotopes as phenotyping tools to assess wheat yield performance: effects of growing temperature and vernalization. Plant Sci. 295, 1–16. https://doi.org/10.1016/j.plantsci.2019.110281.

Rezzouk, F.Z., Gracia-Romero, A., Kefauver, S.C., Nieto-Taladriz, M.T., Serret, M.D., Araus, J.L., 2022. Durum wheat ideotypes in Mediterranean environments differing in water and temperature conditions. Agric. Water Manag. 259, 1–15. https://doi.org/10.1016/j.agwat.2021.107257.

Robbins, N.E., Dinneny, J.R., 2015. The divining root: moisture-driven responses of roots at the micro- and macro-scale. J. Exp. Bot. 66, 2145–2154. https://doi.org/10.1093/jxb/eru496.

Rothfuss, Y., Javaux, M., 2017. Reviews and syntheses: Isotopic approaches to quantify root water uptake: a review and comparison of methods. Biogeosciences 14, 2199–2224. https://doi.org/10.5194/bg-14-2199-2017.

Sanchez-Bragado, R., Serret, M.D., Araus, J.L., 2017. The nitrogen contribution of different plant parts to wheat grains: exploring genotype, water, and nitrogen effects. Front. Plant Sci. 7, 1–14.

Sanchez-Bragado, R., Serret, M.D., Marimon, R.M., Bort, J., Araus, J.L., 2019. The hydrogen isotope composition δ^2H reflects plant performance. Plant Physiol. 180, 793–812. https://doi.org/10.1104/pp.19.00238.

Savin, R., Sadras, V.O., Slafer, G.A., 2019. Benchmarking nitrogen utilisation efficiency in wheat for Mediterranean and non-Mediterranean European regions. Field Crop. Res. 241, 1–7. https://doi.org/10.1016/j.fcr.2019.107573.

Schreel, J.D.M., Steppe, K., 2020. Foliar water uptake in trees: negligible or necessary. ? Trends Plant Sci. 25 (6), 590–603. https://doi.org/10.1016/j.tplants.2020.01.003.
Serret, M.D., Ortiz-Monasterio, I., Pardo, A., Araus, J.L., 2008. The effects of urea fertilisation and genotype on yield, nitrogen use efficiency, $\delta^{15}N$ and $\delta^{13}C$ in wheat. Ann. Appl. Biol. 153, 243–257. https://doi.org/10.1111/j.1744-7348.2008.00259.x.
Slafer, G.A., Andrade, F.H., Feingold, S.E., 1990. Genetic improvement of bread wheat (Triticum aestivum L.) in Argentina: relationships between nitrogen and dry matter. Euphytica 50, 63–71. https://doi.org/10.1007/BF00023162.
Spano, G., Di Fonzo, N., Perrotta, C., Platani, C., Ronga, G., Lawlor, D.W., Napier, J.A., Shewry, P.R., 2003. Physiological characterization of "stay green" mutants in durum wheat. J. Exp. Bot. 54, 1415–1420. https://doi.org/10.1093/jxb/erg150.
Sun, H., Li, J., Song, W., Tao, J., Huang, S., Chen, S., Hou, M., Xu, G., Zhang, Y., 2015. Nitric oxide generated by nitrate reductase increases nitrogen uptake capacity by inducing lateral root formation and inorganic nitrogen uptake under partial nitrate nutrition in rice. J. Exp. Bot. 66, 2449–2459. https://doi.org/10.1093/jxb/erv030.
Thoday-Kennedy, E., Good, N., Kant, S., 2022. Accelerated breeding of cereal crops. In: Bilichak, A., Laurie, J.D. (Eds.), Accelerated breeding of cereal crops. Springer Science+Business Media, LLC, pp. 305–331. https://doi.org/10.1007/978-1-0716-1526-3.
Tian, H., De Smet, I., Ding, Z., 2014. Shaping a root system: regulating lateral versus primary root growth. Trends Plant Sci. 19, 426–431. https://doi.org/10.1016/j.tplants.2014.01.007.
Trachsel, S., Kaeppler, S.M., Brown, K.M., Lynch, J.P., 2013. Maize root growth angles become steeper under low N conditions. Field Crop. Res. 140, 18–31. https://doi.org/10.1016/j.fcr.2012.09.010.
Treydte, K., Boda, S., Graf Pannatier, E., Fonti, P., Frank, D., Ullrich, B., Saurer, M., Siegwolf, R., Battipaglia, G., Werner, W., Gessler, A., 2014. Seasonal transfer of oxygen isotopes from precipitation and soil to the tree ring: source water versus needle water enrichment. N. Phytol. 202, 772–783. https://doi.org/10.1111/nph.12741.
Vadez, V., 2014. Root hydraulics: the forgotten side of roots in drought adaptation. F. Crop. Res. 165, 15–24. https://doi.org/10.1016/j.fcr.2014.03.017.
de Vita, P., Mastrangelo, A.M., Matteu, L., Mazzucotelli, E., Virzì, N., Palumbo, M., Storto, M., Lo, Rizza, F., Cattivelli, L., 2010. Genetic improvement effects on yield stability in durum wheat genotypes grown in Italy. F. Crop. Res. 119, 68–77. https://doi.org/10.1016/j.fcr.2010.06.016.
Wang, P., Song, X., Han, D., Zhang, Y., Liu, X., 2010. A study of root water uptake of crops indicated by hydrogen and oxygen stable isotopes: A case in Shanxi Province, China. Agric. Water Manag. 97, 475–482. https://doi.org/10.1016/j.agwat.2009.11.008.
Wasaya, A., Zhang, X., Fang, Q., Yan, Z., 2018. Root phenotyping for drought tolerance: a review. Agronomy 8, 1–19. https://doi.org/10.3390/agronomy8110241.
Wassenaar, L.I., 1995. Evaluation of the origin and fate of nitrate in the Abbotsford Aquifer using the isotopes of $\delta^{15}N$ and $\delta^{18}O$ in NO_3. Appl. Geochemistry 10, 391–405. https://doi.org/10.1016/0883-2927(95)00013-a.
Wasson, A., Bischof, L., Zwart, A., Watt, M., 2016. A portable fluorescence spectroscopy imaging system for automated root phenotyping in soil cores in the field. J. Exp. Bot. 67, 1033–1043. https://doi.org/10.1093/jxb/erv570.
Wasson, A.P., Richards, R.A., Chatrath, R., Misra, S.C., Prasad, S.V., Sai, Rebetzke, G.J., Kirkegaard, J.A., Christopher, J., Watt, M., 2012. Traits and selection strategies to improve root systems and water uptake in water-limited wheat crops. J. Exp. Bot. 63, 3485–3498. https://doi.org/10.1093/jxb/ers111.
Wasson, A.P., Rebetzke, G.J., Kirkegaard, J.A., Christopher, J., Richards, R.A., Watt, M., 2014. Soil coring at multiple field environments can directly quantify variation in deep root traits to select wheat genotypes for breeding. J. Exp. Bot. 65, 6231–6249. https://doi.org/10.1093/jxb/eru250.
Xynias, I.N., Mylonas, I., Korpetis, E.G., Ninou, E., 2020. Durum wheat breeding in the Mediterranean region: current status and future prospects. Agronomy 10, 1–27. https://doi.org/10.3390/agronomy10030432.
York, L.M., Slack, S., Bennett, M.J., Foulkes, J., 2018a. Wheat shovelomics: phenotyping roots in tillering species. BioRxiv 1–17. https://doi.org/10.1101/280875.
York, L.M., Slack, S., Bennett, M.J., Foulkes, J., 2018b. Wheat shovelomics II: revealing relationships between root crown traits and crop growth. BioRxiv 1–22. https://doi.org/10.1101/280917.
Yousfi, S., Serret, M.D., Araus, J.L., 2009. Shoot δ15N gives a better indication than ion concentration or $\delta^{13}C$ of genotypic differences in the response of durum wheat to salinity. Funct. Plant Biol. 36, 144–155. https://doi.org/10.1111/pce.12055.
Yousfi, S., Serret, M.D., Márquez, A.J., Voltas, J., Araus, J.L., 2012. Combined use of $\delta^{13}C$, $\delta^{18}O$ and $\delta^{15}N$ tracks nitrogen metabolism and genotypic adaptation of durum wheat to salinity and water deficit. N. Phytol. 194 (1), 230–244. https://doi.org/10.1111/j.1469-8137.2011.04036.x.
Zhang, X., Xiao, Y., Wan, H., Deng, Z., Pan, G., Xia, J., 2017. Using stable hydrogen and oxygen isotopes to study water movement in soil-plant-atmosphere continuum at Poyang Lake wetland. China Wetl. Ecol. Manag. 25, 221–234.
Zhao, L., Wang, L., Cernusak, L.A., Liu, X., Xiao, H., Zhou, M., Zhang, S., 2016. Significant difference in hydrogen isotope composition between xylem and tissue Water in Populus Euphratica. Plant Cell Environ. 39, 1848–1857. https://doi.org/10.1111/pce.12753.